Research Paper No.1

to

Office of Naval Research

Detailed Analysis of Hurricane Andrew of 24 August 1992

With Damage Map in Color

ONR Grant N00014-J1136

STORM DATA PROJECT

T. Theodore Fujita, PI

Department of Geophysical Sciences
University of Chicago

AUGUST 1993

Publication delayed 12 months

TABLE OF CONTENTS

Section One

Summary of Research

After learning that south Florida was damaged by Hurricane Andrew, an attempt was made to determine if a damage survey would reveal the existence of expected severe local winds embedded inside the parent circulation.

It has been known for a long time that a number of tornadoes could occur inside a major hurricane. It turned out, however, that most of these hurricane-induced tornadoes occur inside the outer rainbands, rather than the inner rainbands. Of 29 reported tornadoes in Hurricane Allen, which struck southern Texas on 9-11 August 1980, 27 occurred outside the range of 150 km from the hurricane center. It should be noted that 114 tornadoes were mapped inside Hurricane Beulah of 19-23 September 1967 (see Figure 1.1). However, their distribution is seriously questionable. Theoretically, it is possible to find secondary vorticies anywhere inside a parent circulation such as suction vortices inside a tornado. The Beulah-induced tornadoes are too many and erratic to be realistic. It is extremely likely that most of the mapped tornadoes were not tornadoes after all.

Fujita's detailed aerial survey of Andrew revealed that there were a number of embedded circulations. They were carefully examined and identified as "Mini-swirl" and "Microburst" (see Figure 1.2). These mini-swirls and microbursts were found beneath the eyewall cloud (see Figure 1.3). Although the windspeed of these sub-hurricane disturbances is relatively low, say 50 to 100 mph, the total windspeed after adding vectorially the overall hurricane wind could exceed 200 mph. As seen in Figure 1.4, a mini-swirl with an 80 mph rotational wind could induce a 200 mph total wind while traveling at 120 mph.

Pine Woods Villa was damaged seriously by a number of mini-swirls as they moved toward the west-northwest on the right front side of Andrew's eyewall (see Figure 1.5).

Fujita concluded that at least 40 mini-swirls were induced by Hurricane Andrew. Most of these mini-swirls were found within 10 miles of the coastline, suggesting that swirling wind formed while the eyewall circulation after landing was still strong. It is likely that mini-swirls formed beneath strong updrafts which provide significant stretching motion at the surface.

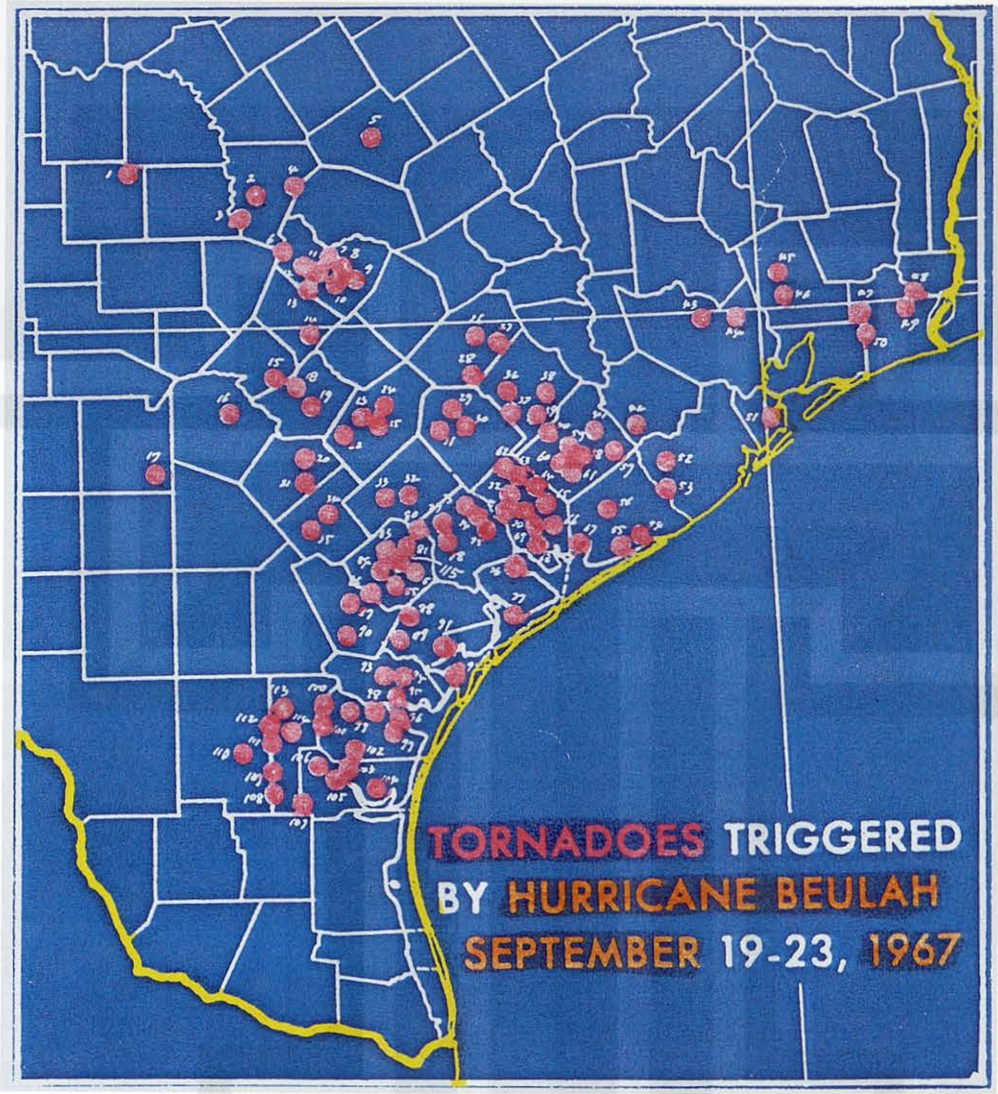

Fig. 1.1 One hundred fourteen (114) tornadoes mapped inside Hurricane Beulah of 19-23 September 1967. The number is extremely large to be meteorologically acceptable.

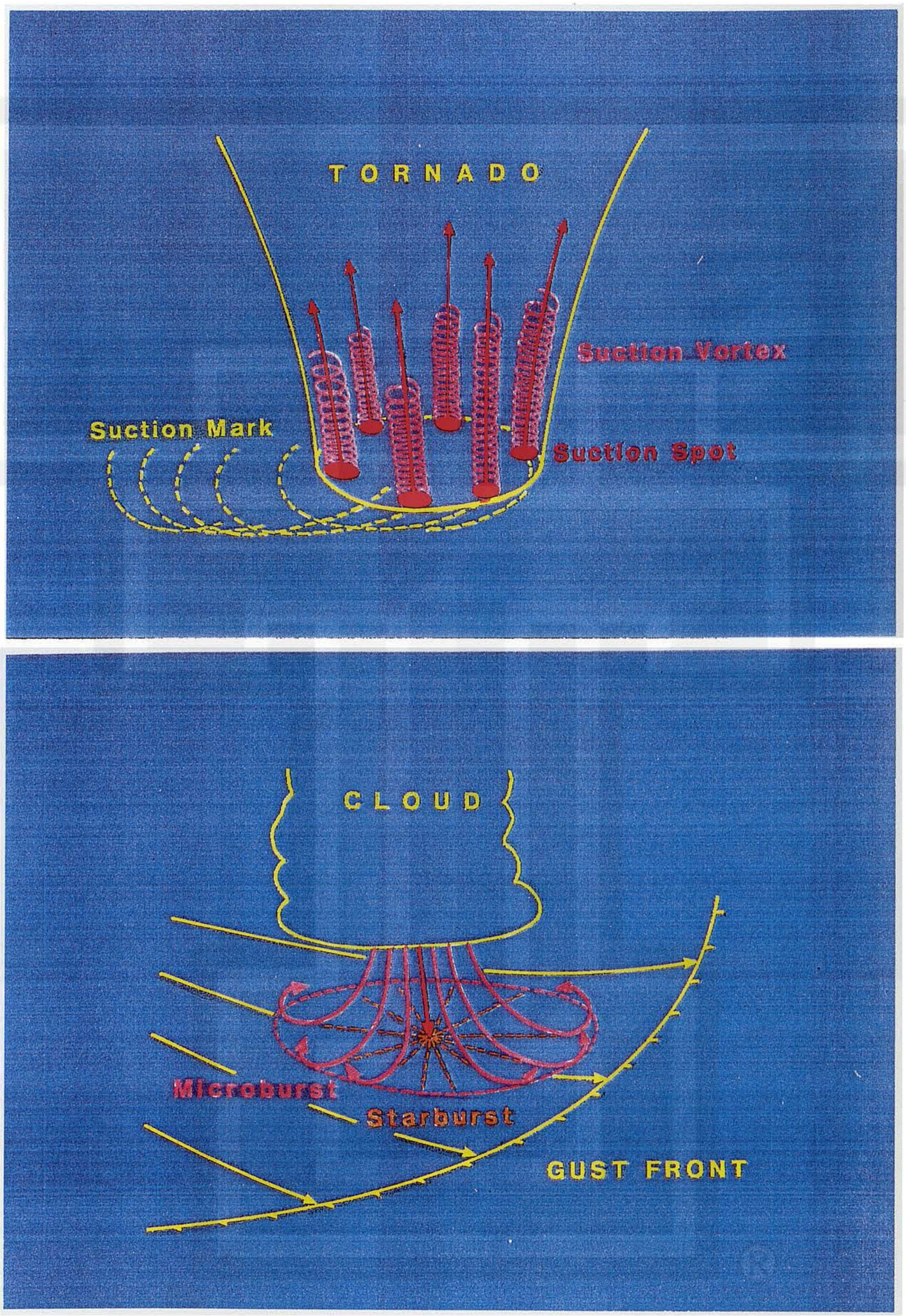

Fig. 1.2 Schematic views of a large tornado with suction vortices (top) and a microburst (bottom). No tornado was confirmed inside Andrew, but suspected microburst damage was found.

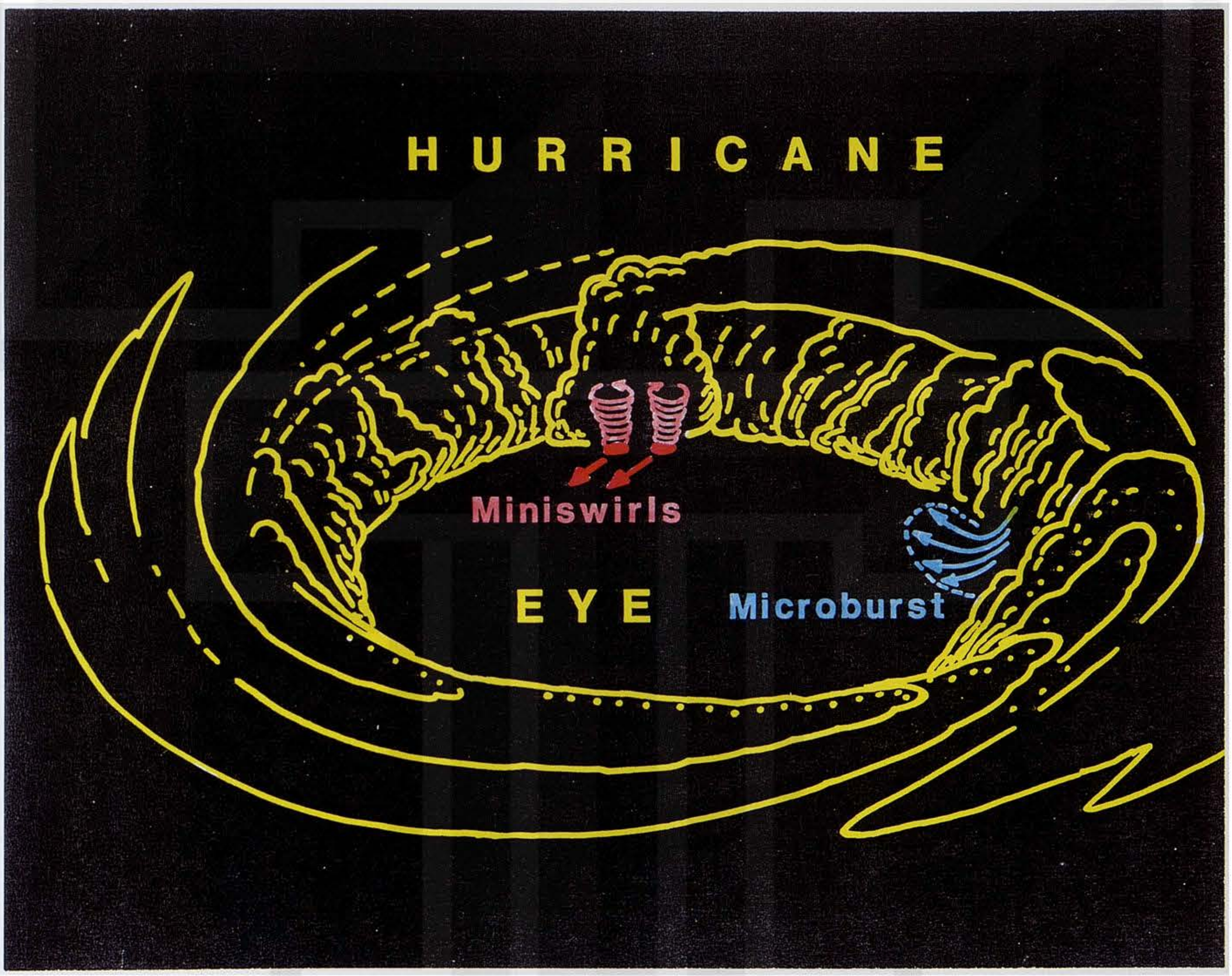

Fig. 1.3 Mini-swirls and a microburst located beneath a hurricane eyewall cloud. These small-scale winds could induce severe local damage at various locations.

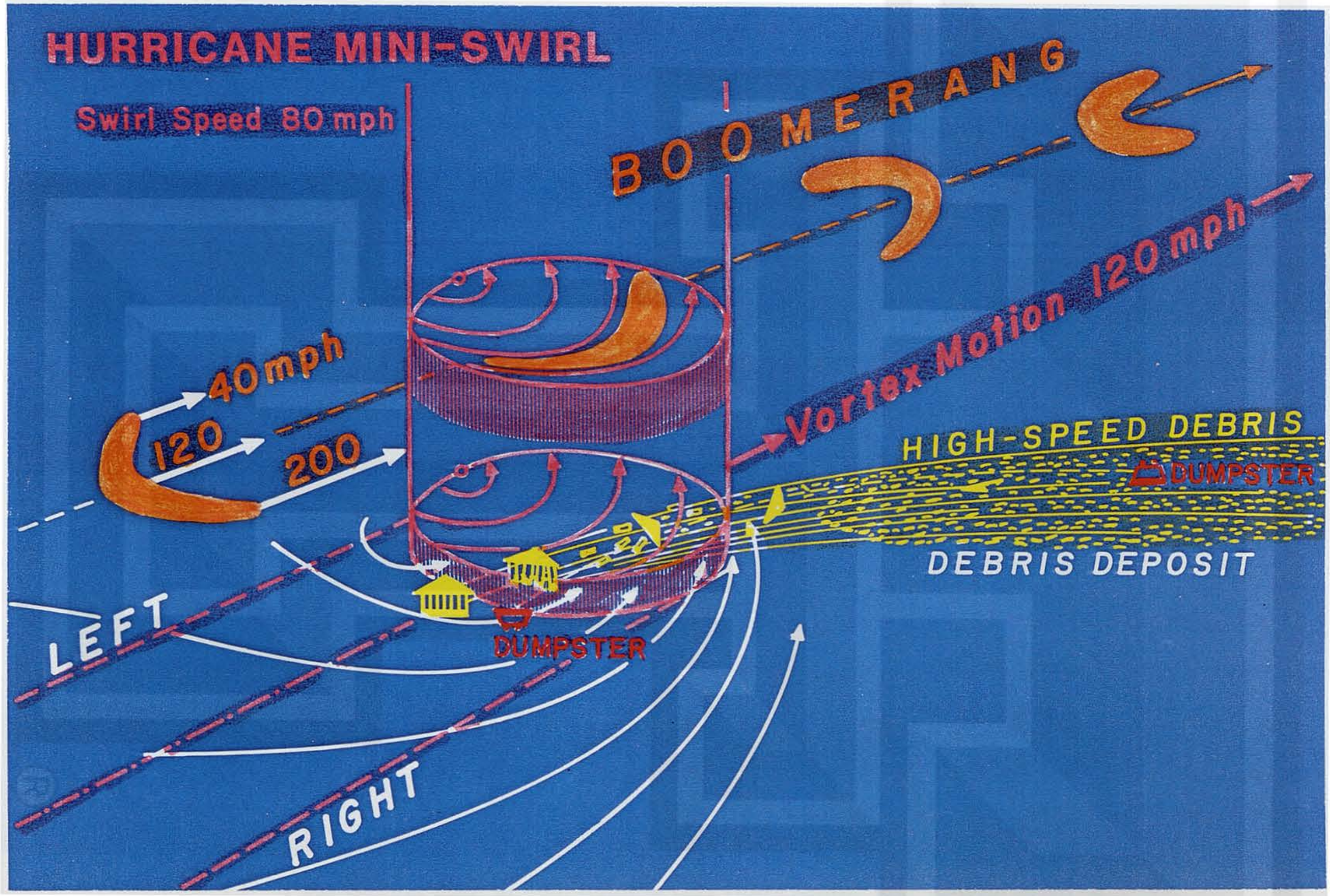

Fig. 1.4 A hurricane mini-swirl could induce a 200 mph wind by virtue of its fast translational motion, like a boomerang.

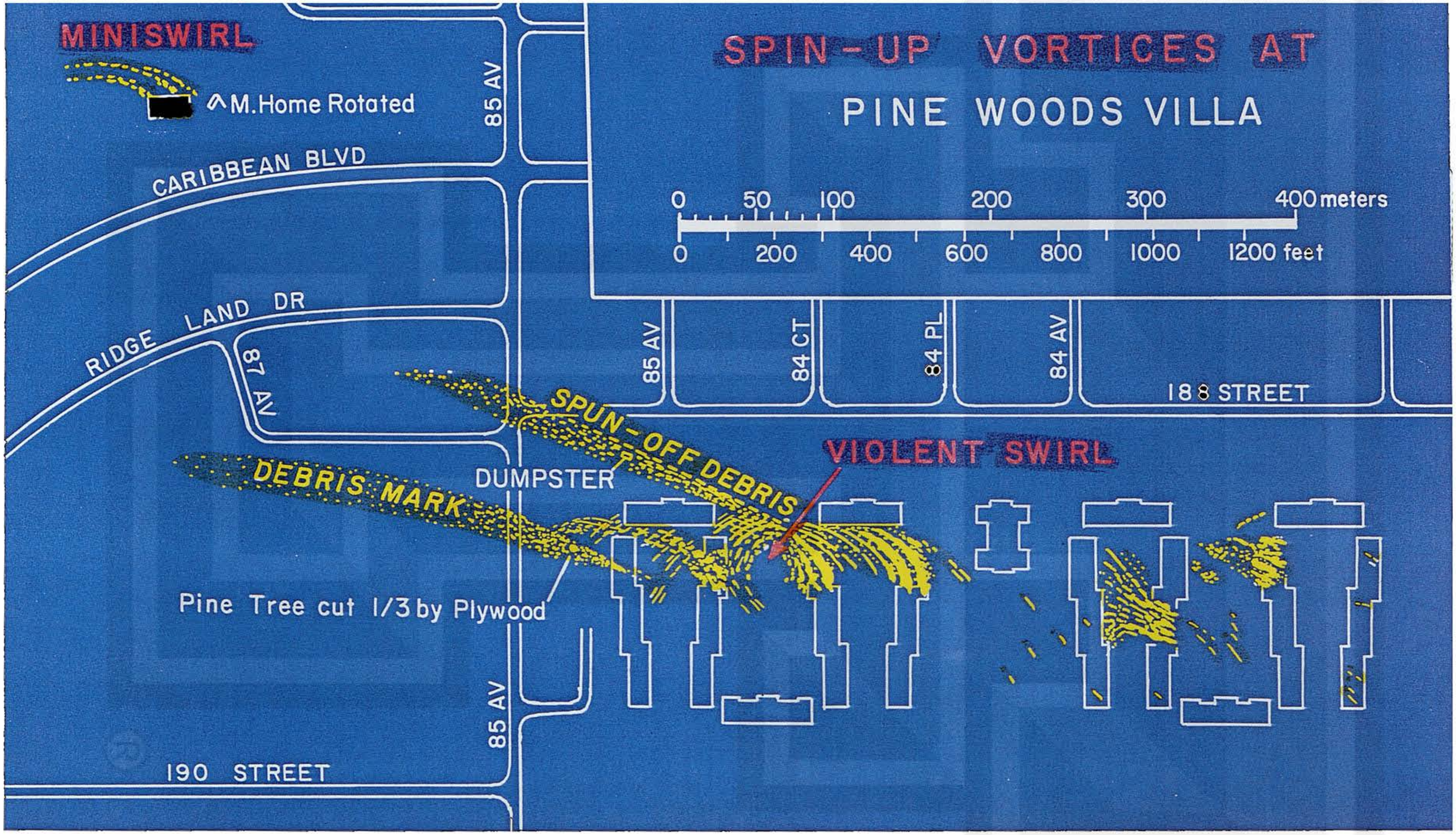

Fig. 1.5 Pine Woods Villa, at 85th Avenue and 188th Street, was broken apart. A dumpster was found inside a streak of debris. The estimated peak wind was 200 mph.

Section 2

Movement of Radar Echoes

Due to the inavailability of barograph traces from the core region of Andrew, an attempt was made to estimate the pressure profile from the reported minimum pressures. Figure 2.1 presents the distribution of minimum pressures measured at various locations. Some were only 5 km or less from the coastline (shown in green), while others were over 5 km from the coastline. Since the estimated minimum central pressure at landing was 925 mb, very strong circulation was expected.

Rotational winds of Andrew between 8:45 and 10:14 UTC (EDT + 4 hours) were depicted by the radar echo motion during approximate 10-minute periods. Initial times of each period are identical to the photo time indicated on each of the Key West radar pictures in Figures 2.2 through 2.8

The sequence of radar-echo motions shown in Figures 2.2 through 2.8 demonstrates that such inferred winds are very useful in assessing the overall circulation which could not be determined from surface anemometers. Only one anemometer at the National Hurricane Center recorded windspeeds during Andrew.

While Andrew's fury and damage were occurring on the ground, USAF C-130 weather aircraft penetrated the storm at 10,000 feet three times in the north-south direction. The first traverse was from south to north, flying around inside the eye between 4:03 a.m. and 4:06 a.m. EDT. The second traverse was from north to south, penetrating the eye at 5:21 a.m. EDT. The third penetration was from south to north, circling inside the eye between 6:07 and 6:14 a.m. EDT.

Shown in Figures 2.9 and 2.10 are the second and third traverses of the eye by the C-130 aircraft. The aircraft encountered both up and downdrafts while inside the eyewall clouds.

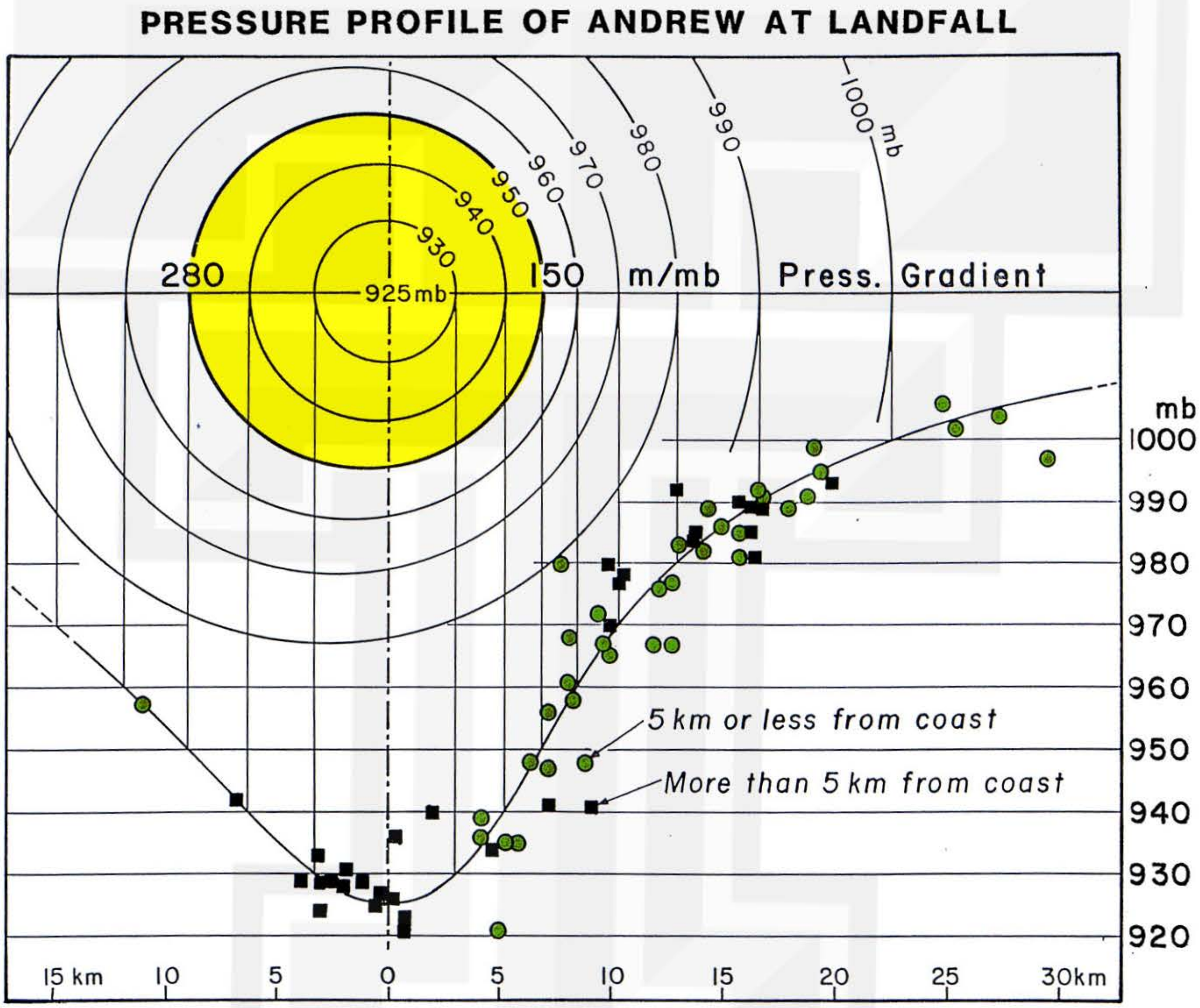

Fig. 2.1 Estimated pressure profile of Andrew as it landed in south Florida and moved inland. The lowest sea-level pressure was 925 mb.

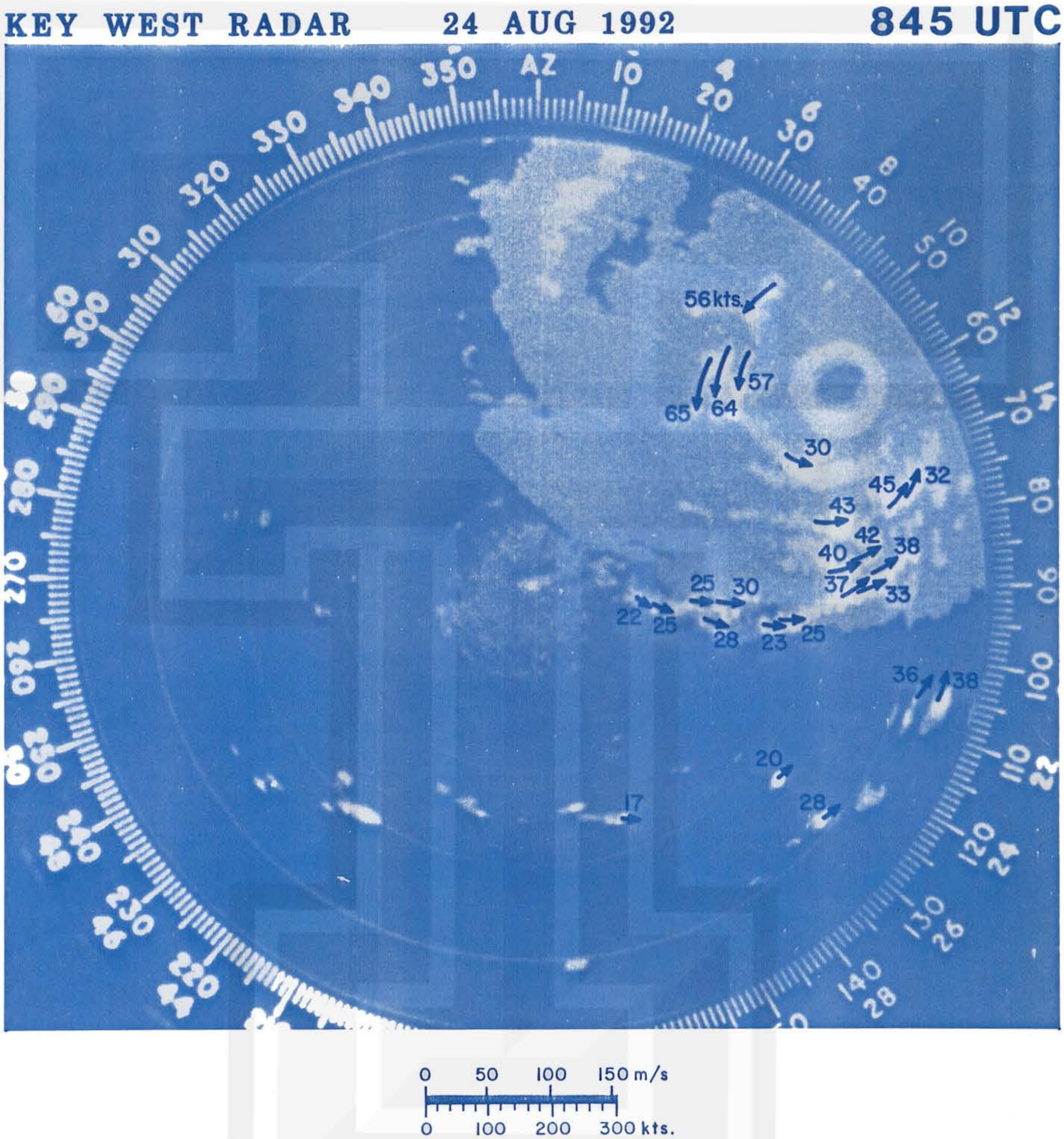

Fig. 2.2 Radar echo motion during the 9-minute period, 8:45 to 8:54 UTC, superimposed on the initial image of the analyzed sequence. As can be seen, echo motion is useful to infer windspeed, however it is limited by the availability of traceable tags. The maximum echo motion observed is 65 knots, about 30 nm due west of the hurricane's center.

KEY WEST RADAR 24 AUG 1992 **854 UTC**

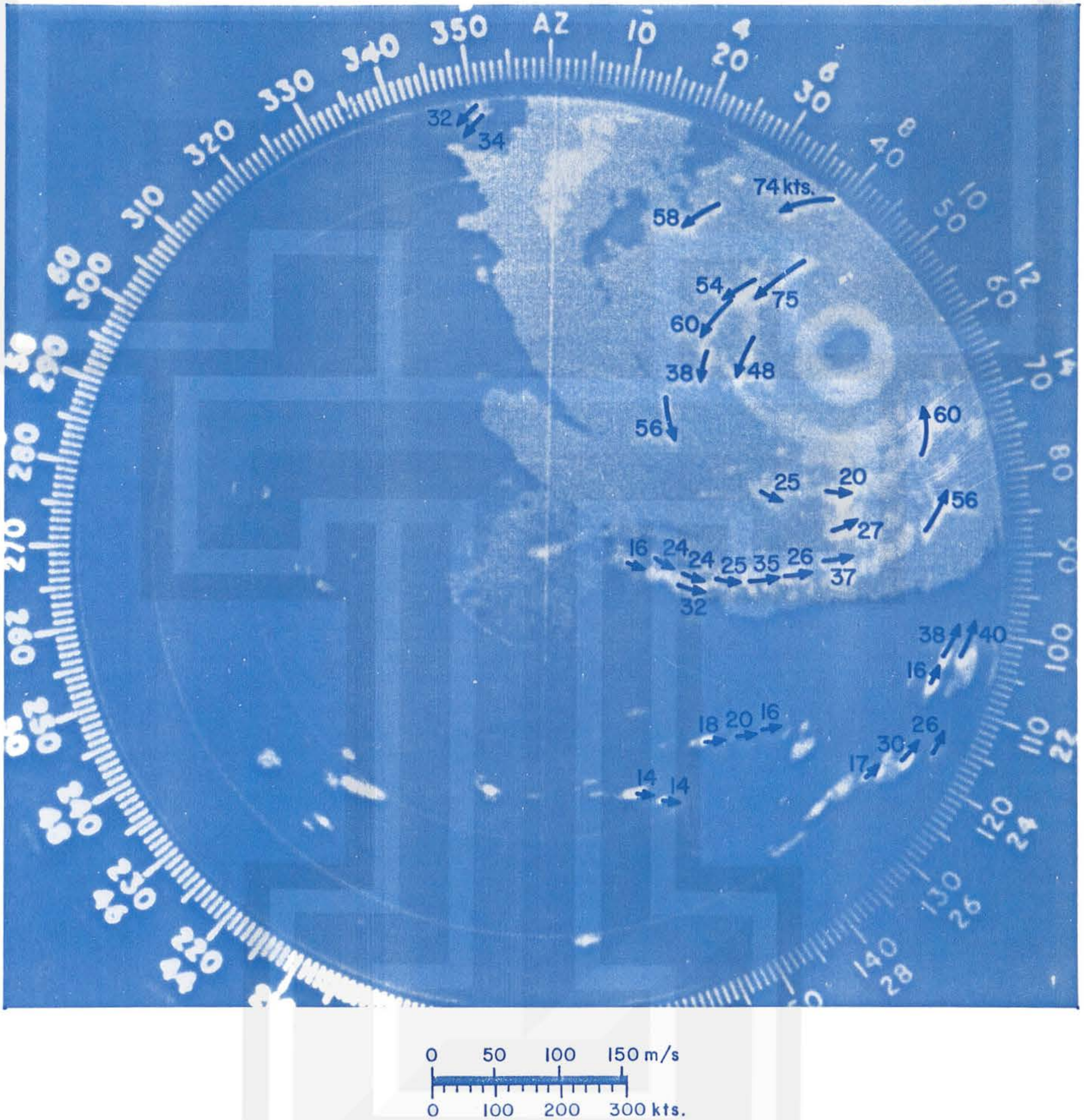

Fig. 2.3 Radar echo motion during the 10-minute period, 8:54 to 9:04 UTC, superimposed on the 8:54 UTC image. The maximum echo motion observed is 75 knots about 25 nm northwest of the storm center. Note that in all of the analyses (Figures 2.2 through 2.8) the maximum echo motion is consistently observed in the right front quadrant of the storm.

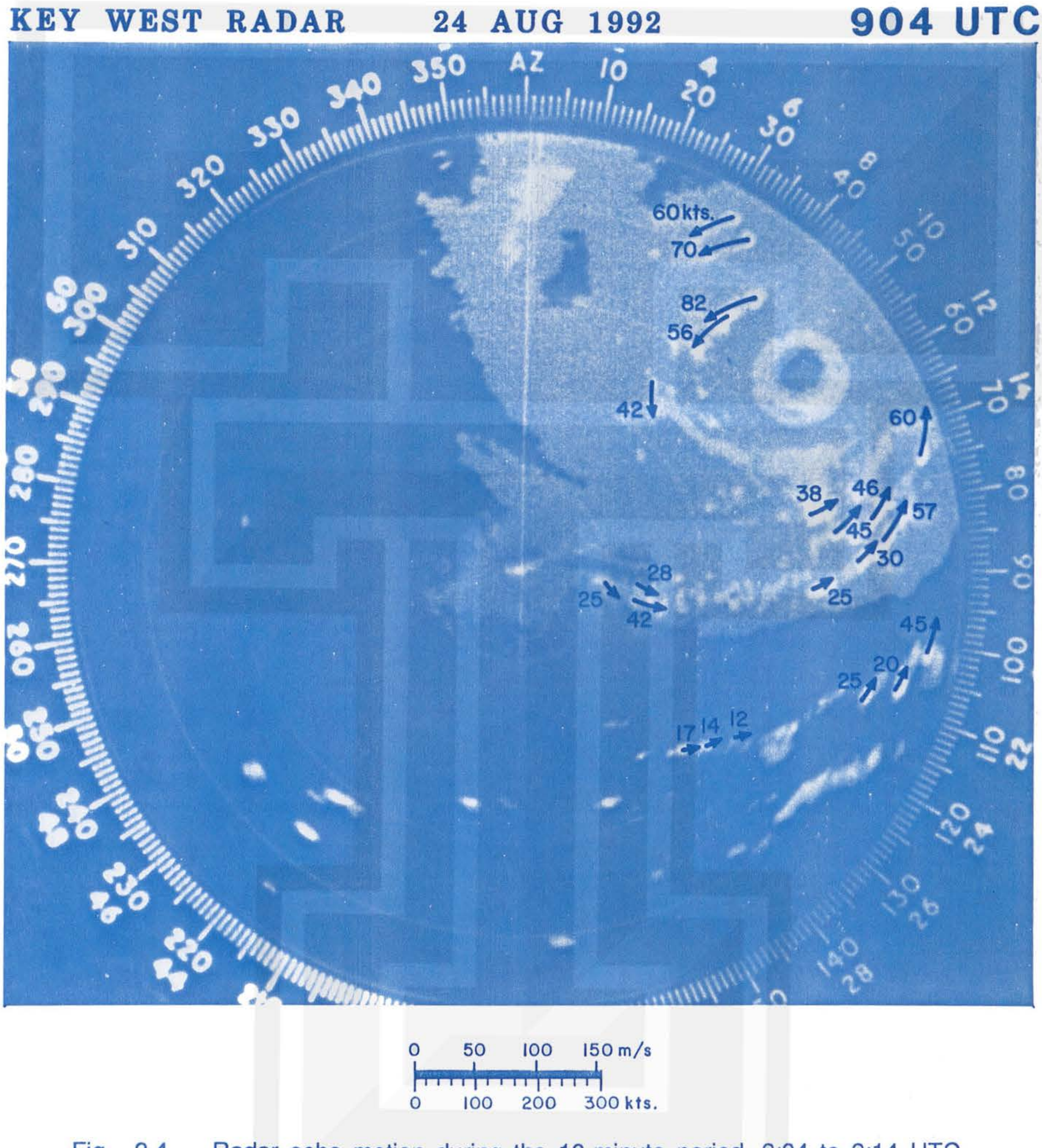

Fig. 2.4 Radar echo motion during the 10-minute period, 9:04 to 9:14 UTC, superimposed on the 9:04 UTC image. The maximum of 82 knots is about 25 nm northwest of the storm center.

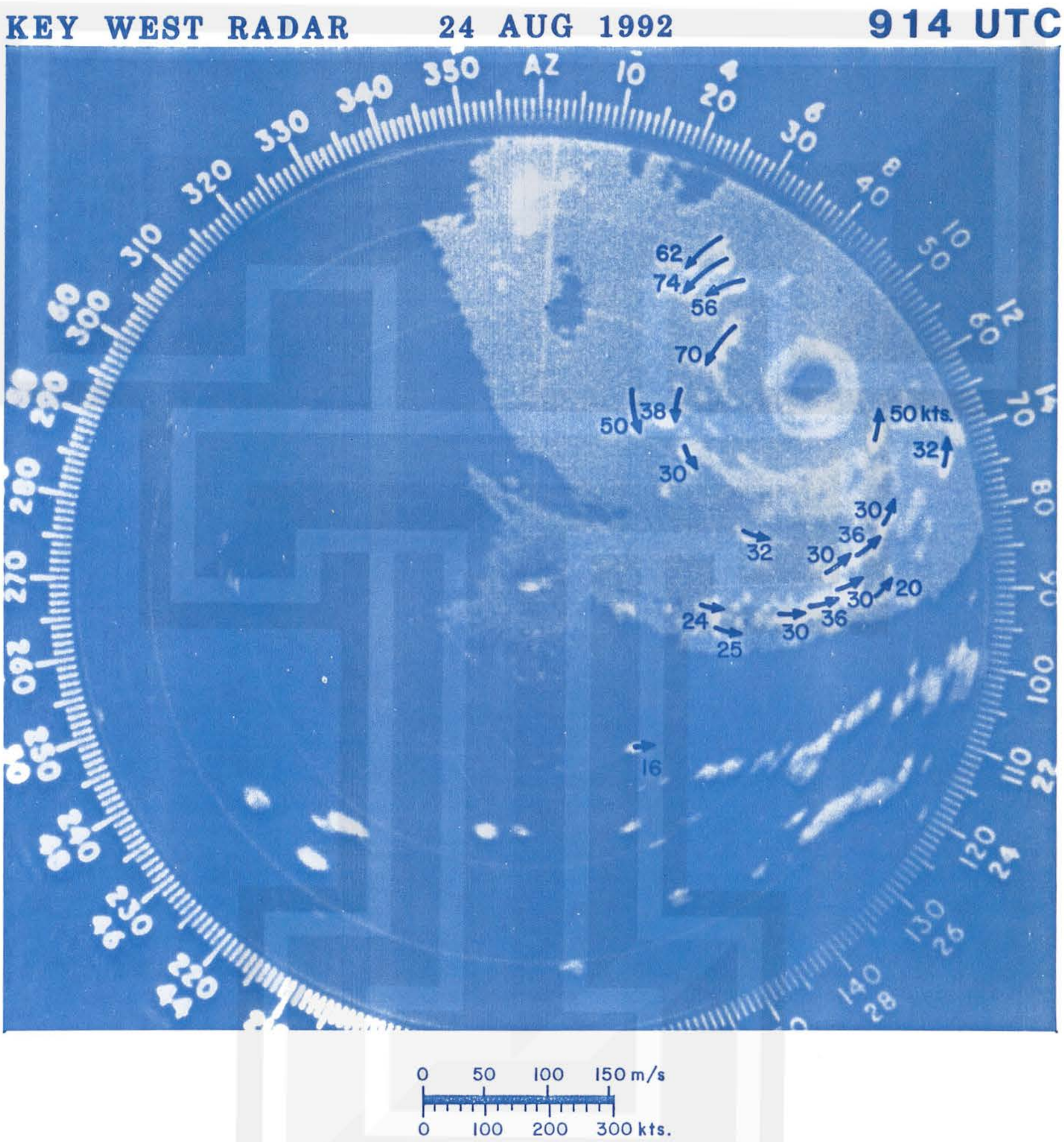

Fig. 2.5 Radar echo motion during the 9-minute period, 9:14 to 9:23 UTC, superimposed on the 9:14 UTC image.

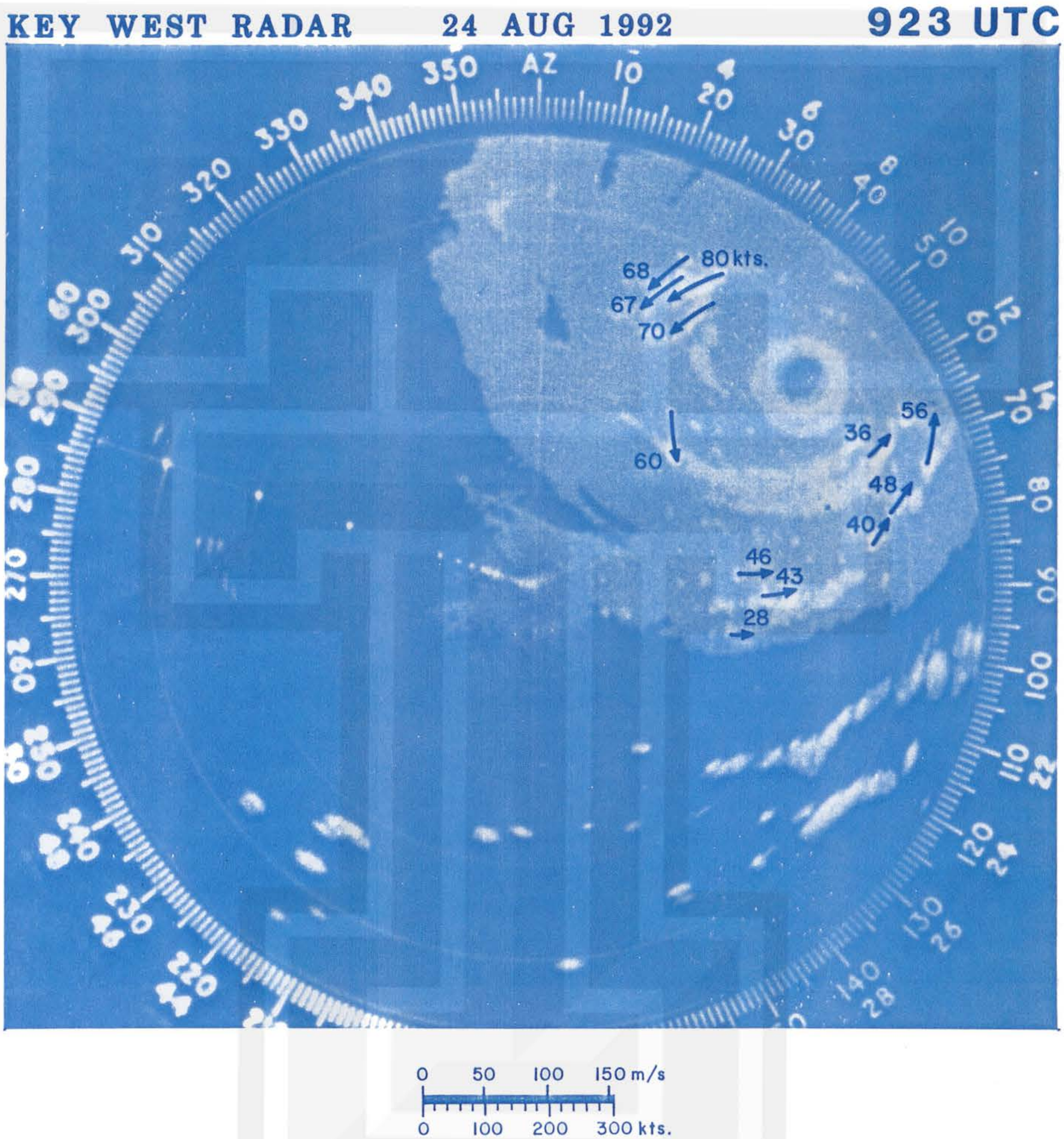

Fig. 2.6 Radar echo motion during the 12-minute period, 9:23 to 9:35 UTC, superimposed on the 9:23 UTC image.

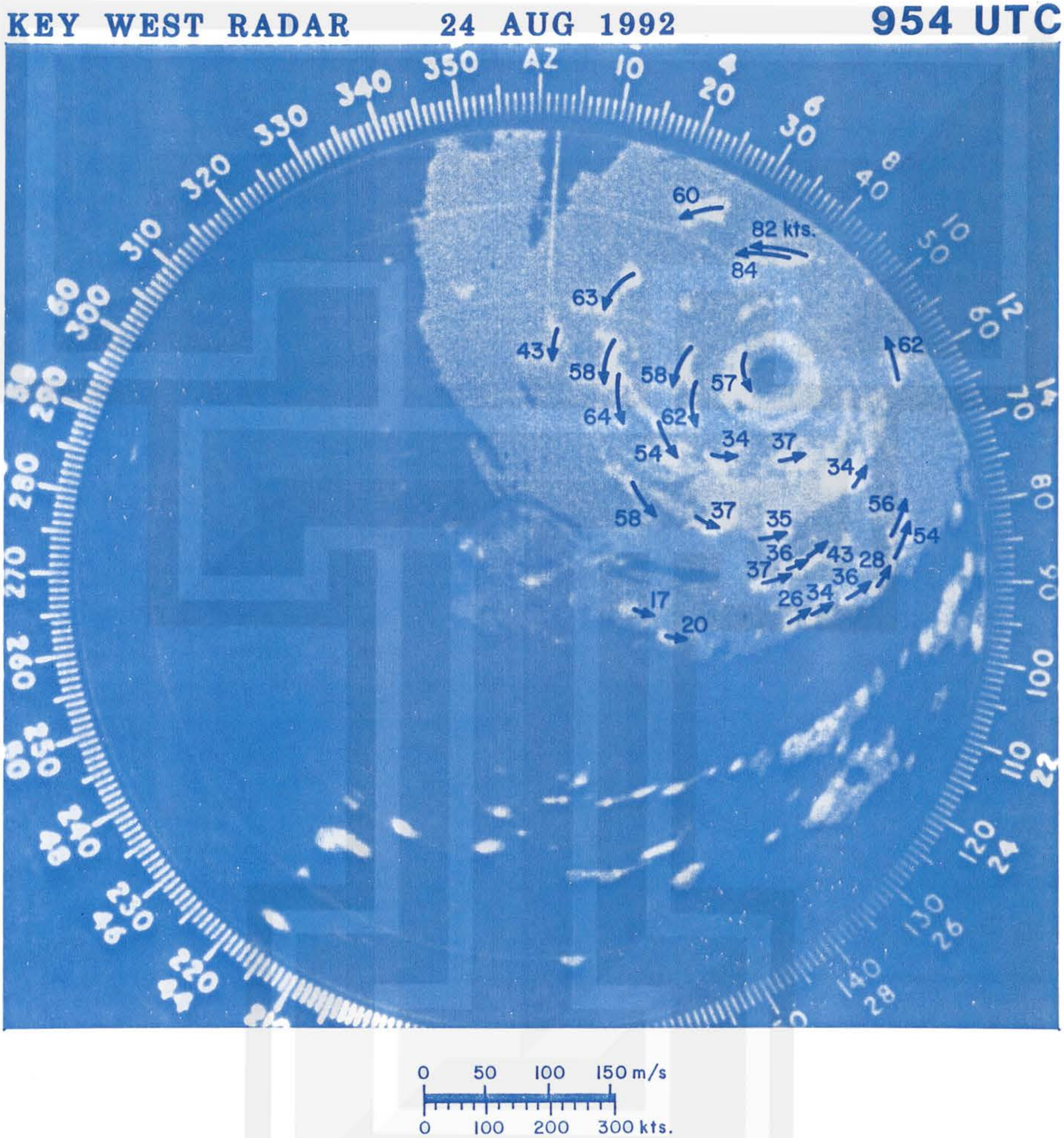

Fig. 2.7 Radar echo motion during the 10-minute period, 9:54 to 10:04 UTC, superimposed on the 10:04 UTC image. The maximum of 84 knots is the highest observed in all of the seven analysis periods.

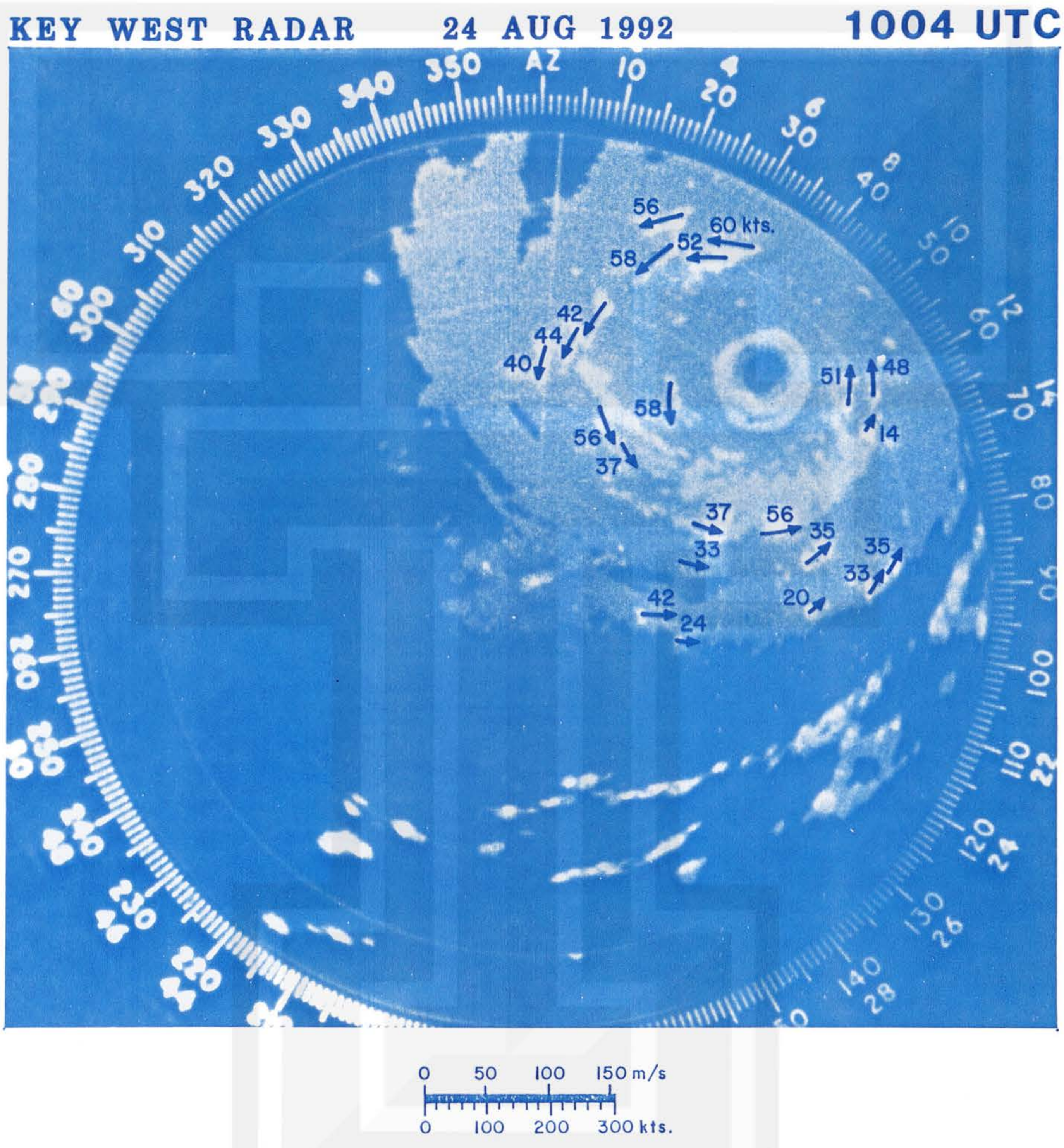

Fig. 2.8 Radar echo motion during the 10-minute period, 10:04 to 10:14 UTC, superimposed on the 10:14 UTC image.

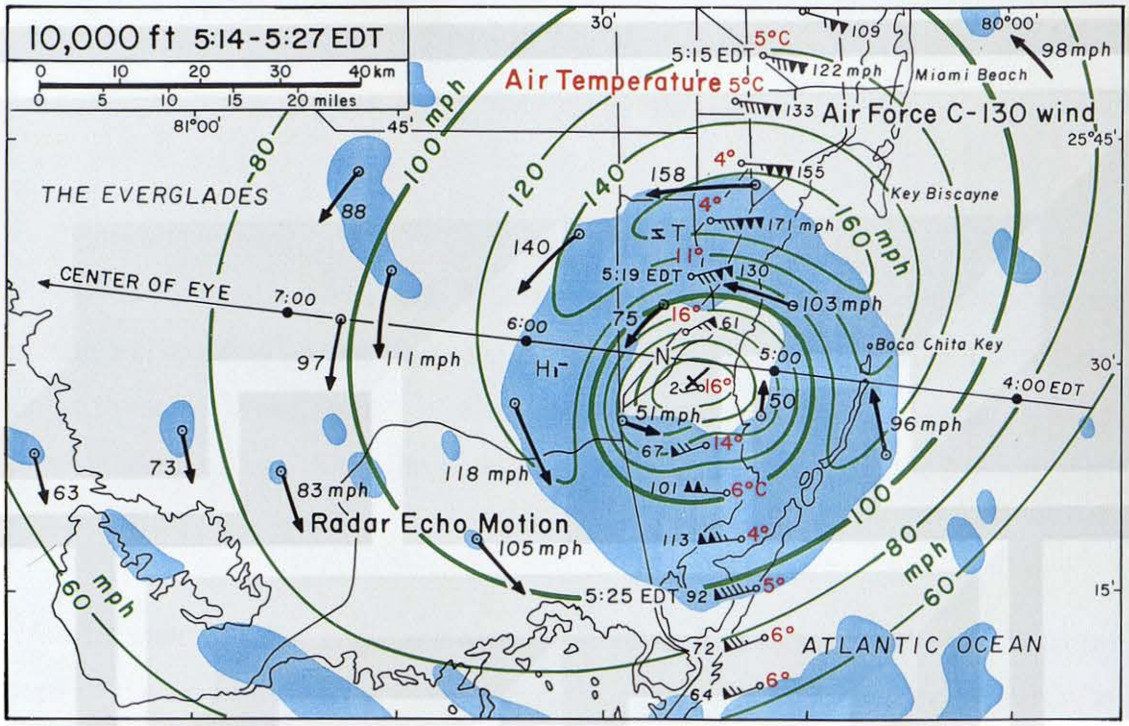

Fig. 2.9 The second traverse of Andrew's eye, between 5:17 and 5:25 EDT, by USAF C-130 aircraft.

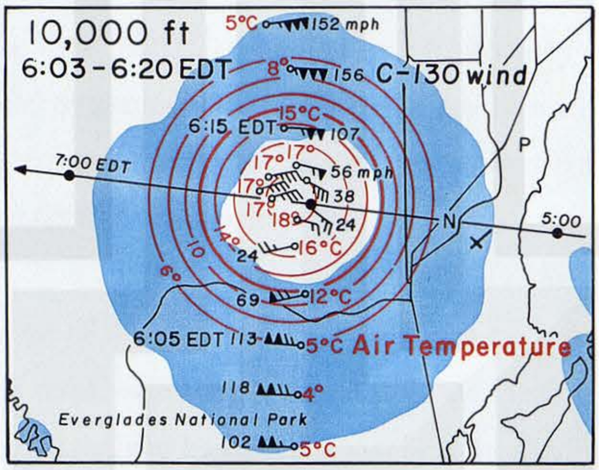

Fig. 2.10 The third traverse of Andrew's eye, between 6:03 and 6:17 EDT, by USAF C-130 aircraft.

Section Three

First and Second Winds

First and second winds are defined, respectively, as those blowing during approaching and receding phases of the eye of a circular wind system, such as a hurricane, typhoon or tornado. When the eye of such a storm passes over an anemometer, a sharp drop in windspeed occurs. After the passage of the eye, the speed of the second wind increases rapidly.

Unfortunately, not a single anemometer in south Florida recorded both direction and speed of the first and second winds during the passage of Andrew's eye. Shown in Figure 3.1 are anemometer traces recorded by the Naval Air Station (NAS) and National Weather Service (NWS) station in Guam during the passage of Typhoon Omar on 28 August, four days after the landfall of Hurricane Andrew in south Florida.

Fujita estimated the flow pattern of Andrew's first winds by determining the fall directions of either uprooted or snapped trees of approximate 10-meter height. As shown in Figure 3.2, the flow pattern is similar to the expected inflow pattern. Converging flows are seen along the shoreline north of the hurricane center.

The damage direction of Andrew's second wind was hard to determine because most of the damageable tall trees were already downed during the first wind. The damage vectors in Figure 3.3 were determined by carefully mapping sand drift and the streaks of plastic covers from large numbers of greenhouses scattered in south Florida.

The angle of windshift between the first and second winds is mapped in Figure 3.4. The line of 180° shift extends along and near the path of the eye center. A clockwise shift with +150° to +90° shift angles occured to the north, and -150° to -90° counterclockwise shift angles are seen to the south.

Both first and second winds were mapped inside a large area extending into the Everglades. Unexpectedly, three (3) areas of strong first winds were identified — in the Everglades, near Homestead Air Force Base, and in Homestead (see green areas in top panel of Figure 3.5). Similar areas, identified as 4, 5 and 6 in the lower panel of Figure 3.5, were located in the second winds. This evidence denotes that there were localized high winds inside Andrew, creating damage swaths 2 to 7 miles wide and 5 to 15 miles long. Windspeeds in these areas were estimated to be 20 to 30 mph higher than the overall Andrew winds of 140 mph. The force of the resultant wind is proportional to the square of the total wind, $(140 + 30)^2 = 1.47 \times 140^2$, or approximately 50% larger. The difference in damage caused by 140 mph and 170 mph winds can be identified easily in aerial photographs.

Finally, first- and second-wind patterns of Hurricane Andrew were superimposed upon the island of Oahu, centered at Pearl Harbor. In Oahu, however, the effects of downslope must be taken into consideration in assessing the wind damage. It is known that downslopes in hurricanes accelerate wind, resulting in Boulder-type high winds.

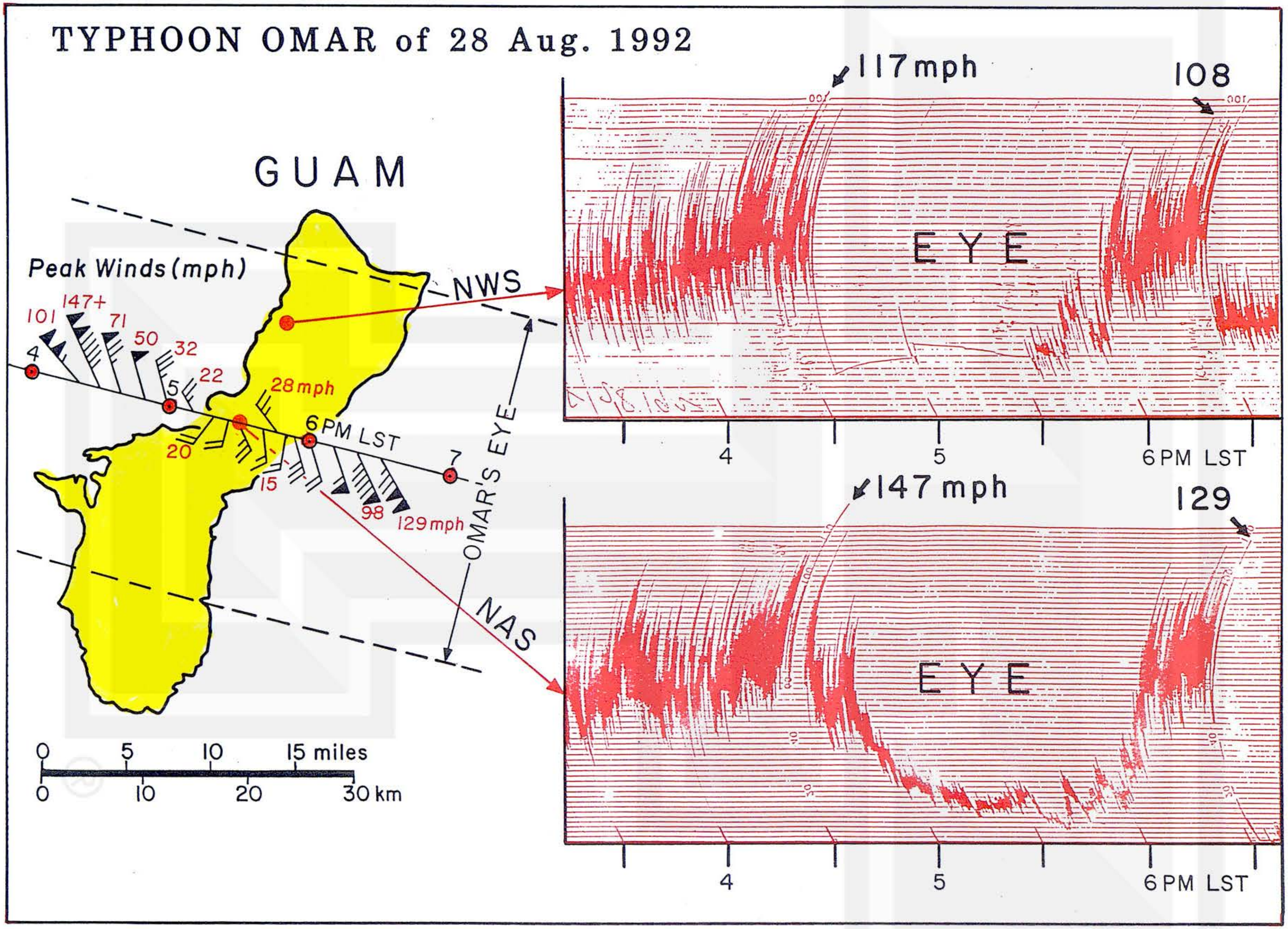

Fig. 3.1 First and second winds recorded by two anemometers in Guam during the pasage of Typhoon Omar of 28 August 1992.

First Winds (10m Winds)

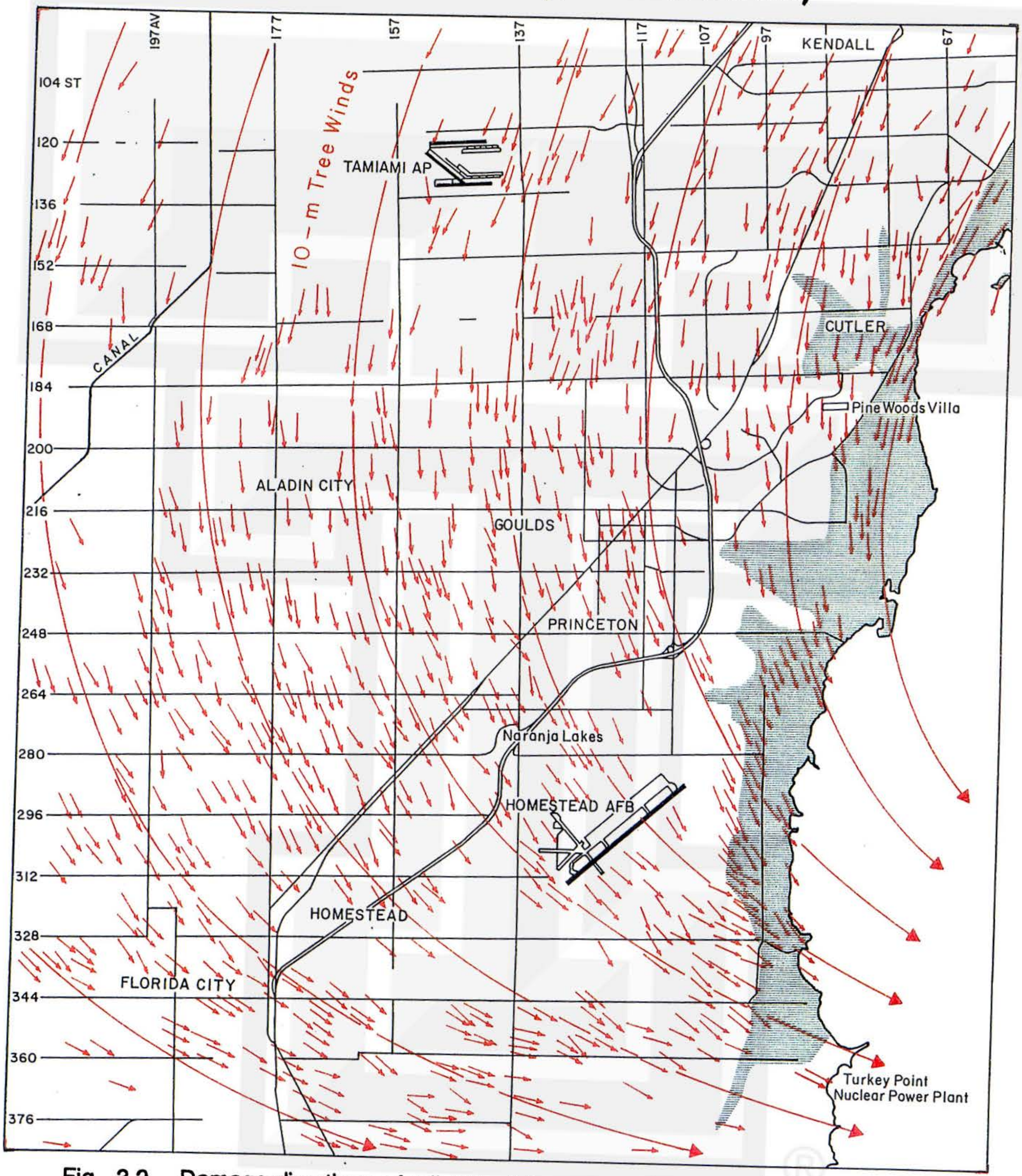

Fig. 3.2 Damage directions of tall (10 m) trees occurring during the first wind of Hurricane Andrew.

Second Winds (1m & 10m Winds)

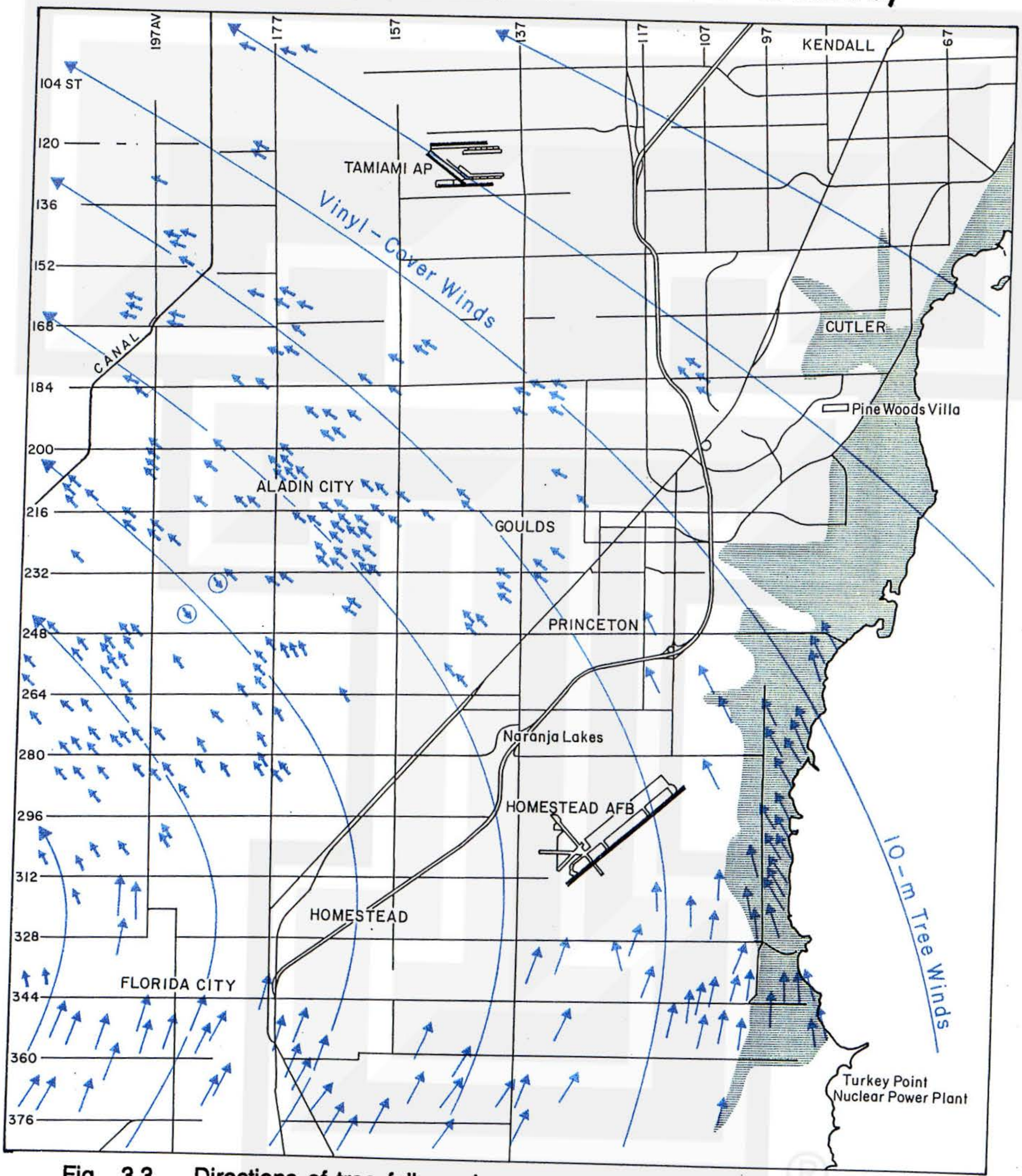

Fig. 3.3 Directions of tree falls and near-ground streaks occurring during the second wind of Andrew.

Wind-Shift Isogons

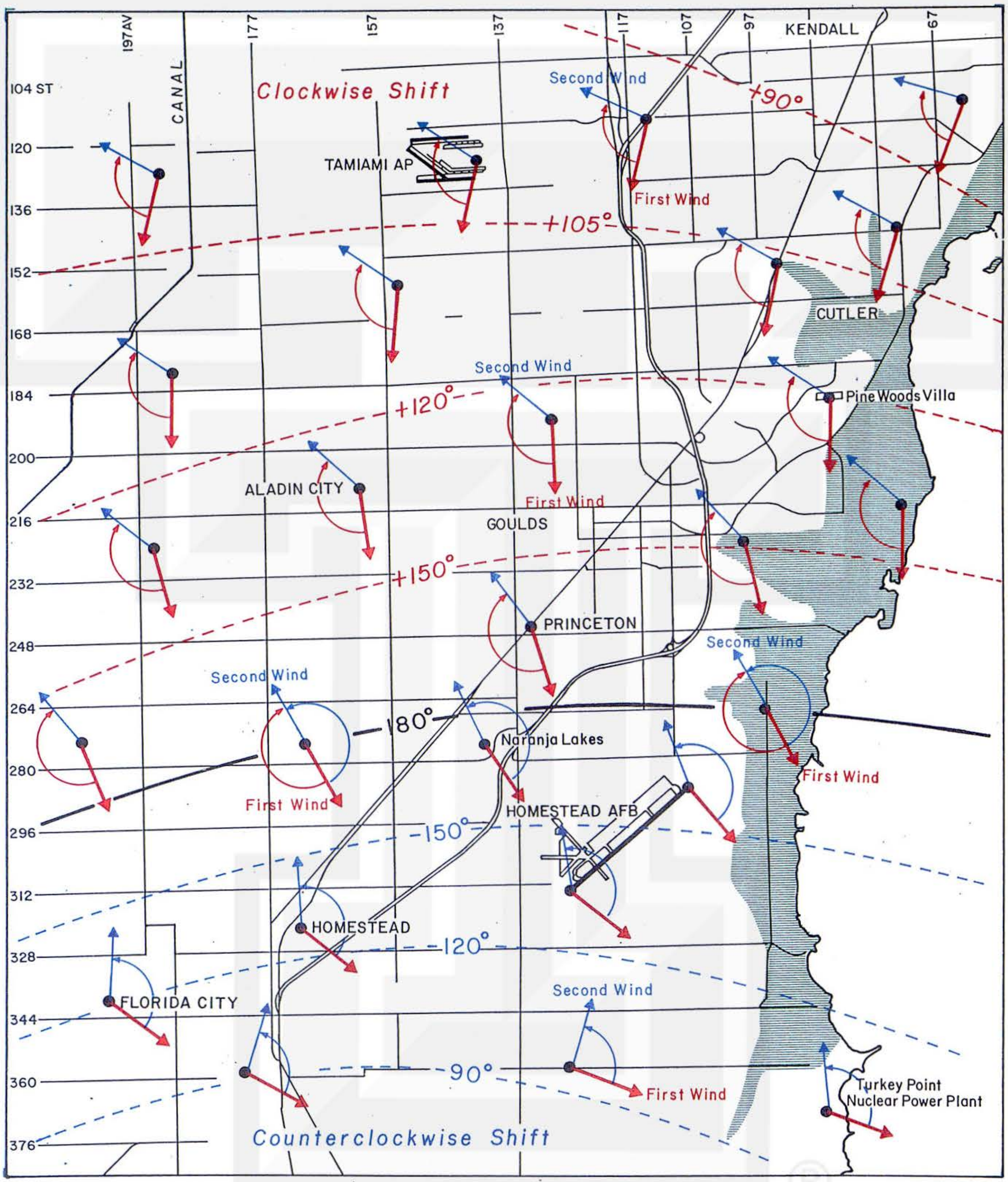

Fig. 3.4 Vector shift of the first wind into the second wind during the approaching-receding changeover phase of Andrew's eye as it passed across southern Florida.

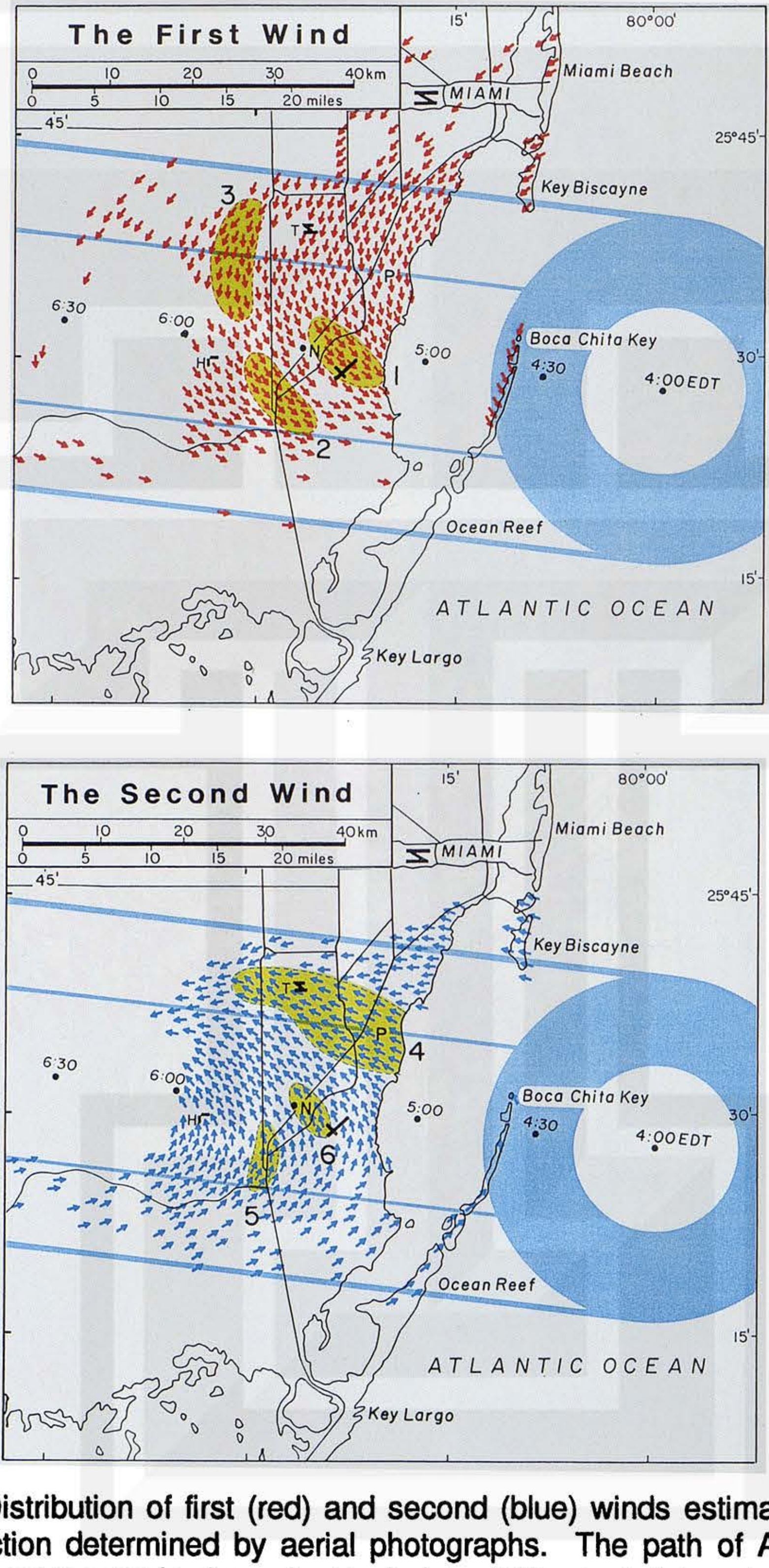

Fig. 3.5 Distribution of first (red) and second (blue) winds estimated from the damage direction determined by aerial photographs. The path of Andrew's eye moving from east to west is shown by black dots at 30-minute intervals.

ANDREW'S WINDS CENTERED at PEARL HARBOR

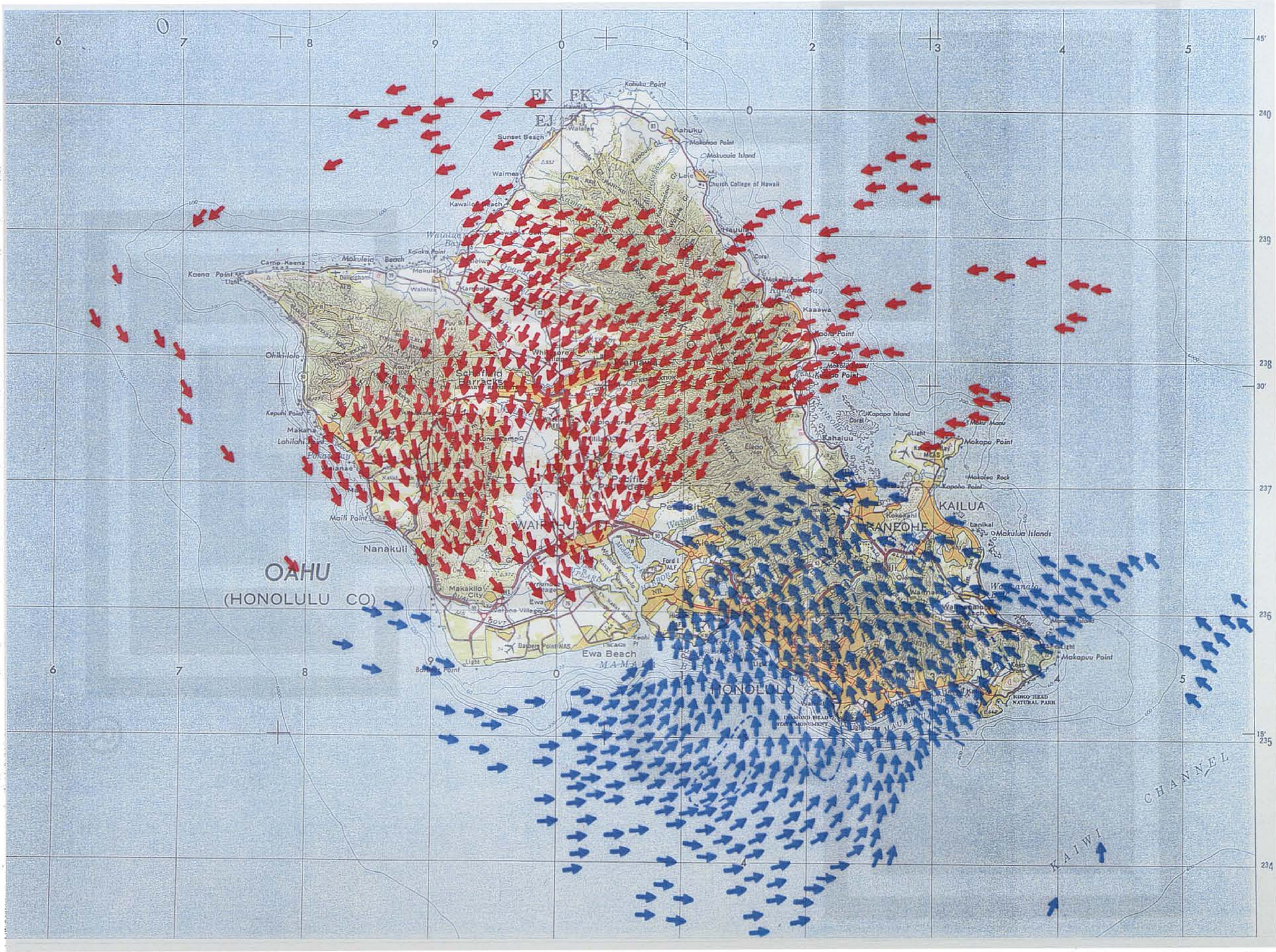

Fig. 3.6 First (red) and second (blue) winds of Hurricane Andrew superimposed upon the island of Oahu when the hypothetical eye would be passing over Pearl Harbor.

Section Four

Contribution to Storm Data

At the request of NOAA, Fujita contributed the following Hurricane Andrew article and damage map in color to Storm Data; August 1992 issue, pages 21-25.

Damage Survey of Hurricane Andrew in South Florida by Ted Fujita

The vast areas of south Florida damaged by Hurricane Andrew on 24 August were mapped by Fujita based on his 500 high-resolution aerial photos and 1,500 9" X 9" vertical aerial photos purchased from Continental Aerial Survey, Pan American Survey and Aerial Cartographics of America.

Three scales of wind systems were isolated and studied in detail. They are (1) Overall hurricane, (2) Swath of high wind, and (3) Mini-swirl and microburst. The damage-causing peak winds of (2) and (3) were far stronger than ordinary peak gusts experienced along the path of Andrew.

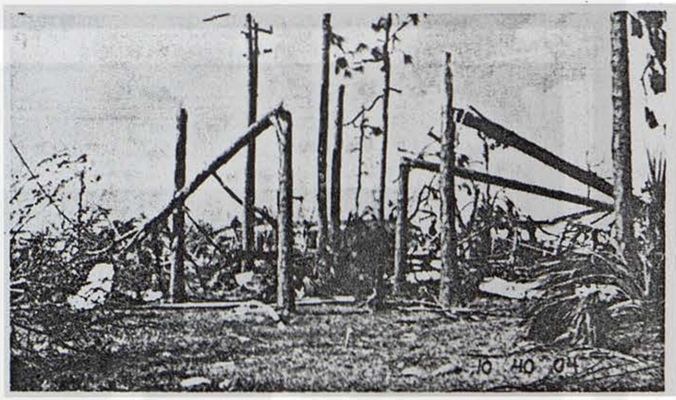

Typical damage of pine trees caused by the first and second winds. Numerous Australian pines were blown down by the first wind. Fujita photo 1040 EDT 9/9/92

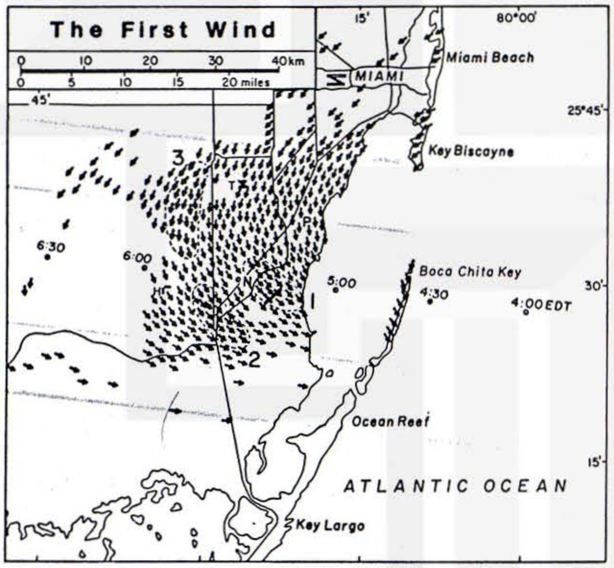

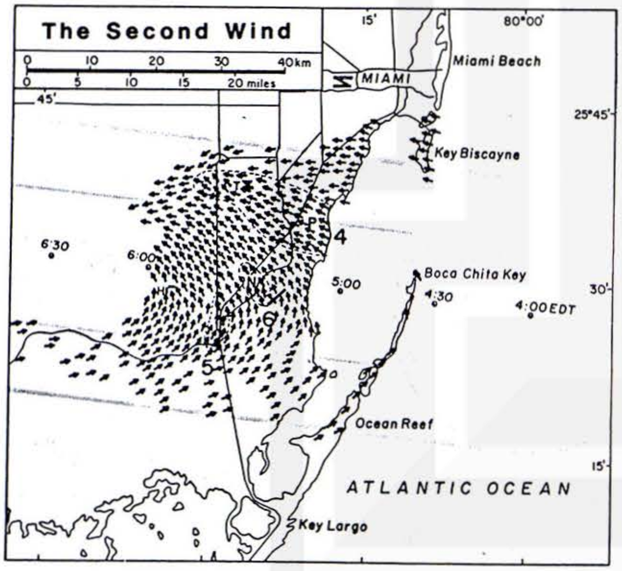

Above: Direction of the first damaging wind occurring during the approach phase of Andrew. **Below:** Damage by the second wind, during the receding phase.

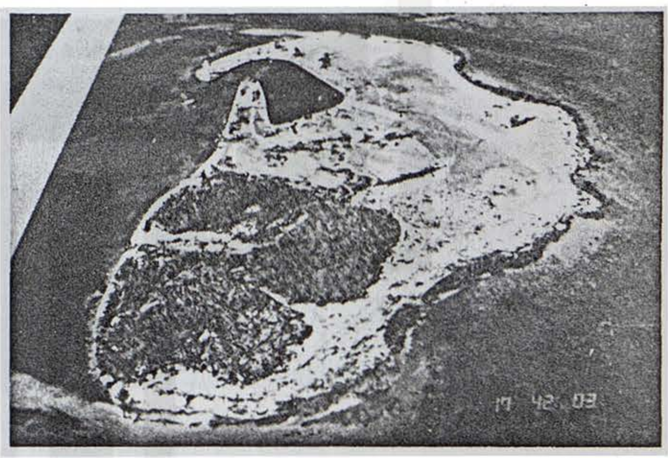

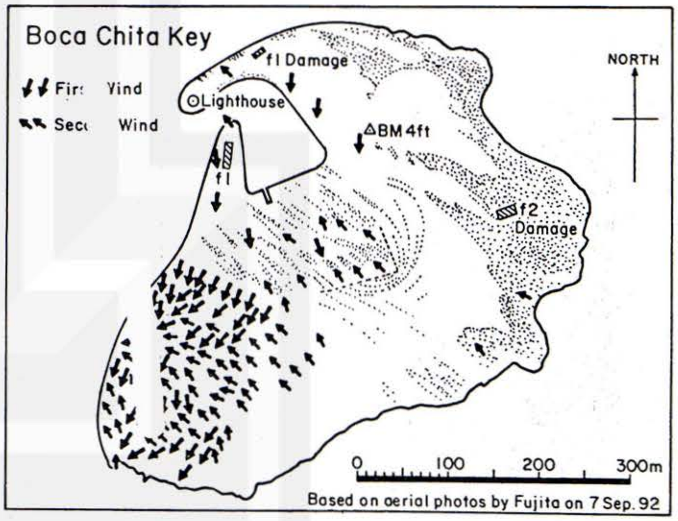

Above: Boca Chita Key, 2 to 3 miles north of the eye center, received the first storm fury. Fujita photo 1742 EDT 9/7/92. **Below:** Damage map showing the average direction of the first wind from 10° and the second wind from 125°.

Mini-swirl Damage at Pine Woods Villa Southeast of 188 St and 87 Av SW

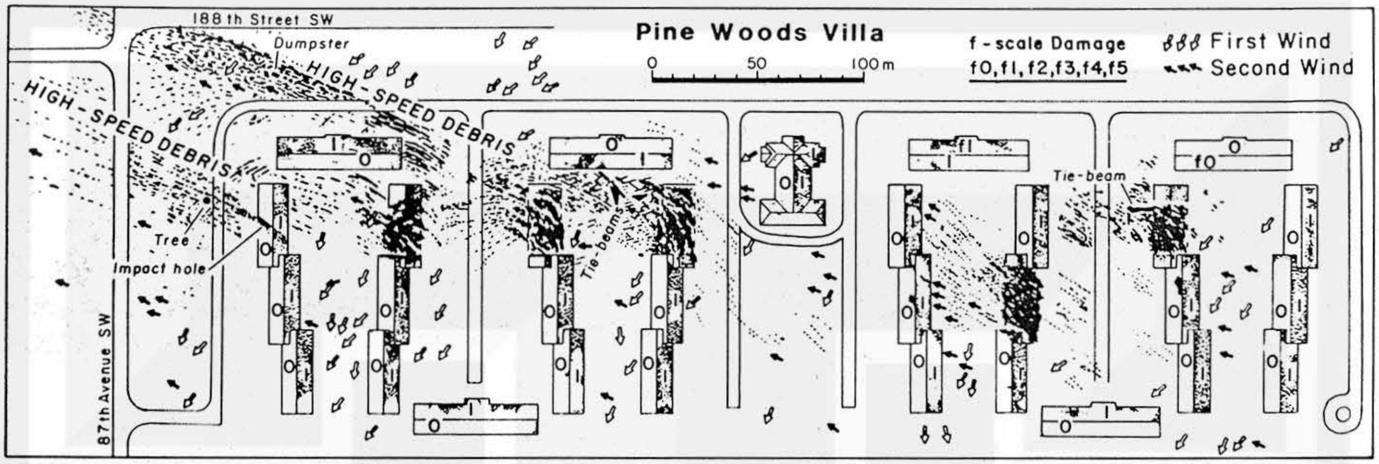

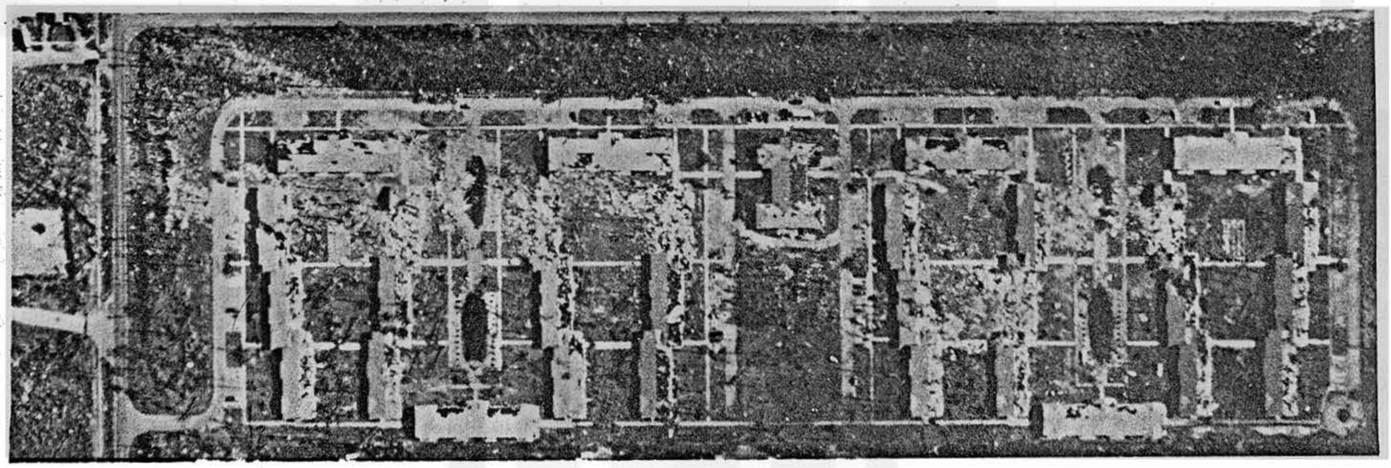

Above: Structural and tree damages at the Villa located inside the Tamiami Swath. Although trees were damaged by both first and second winds, the first wind did not cause structural damage, suggesting that the first wind was weaker than the second wind in the Tamiami Swath. The second wind caused the f1 damage to the east-side roofs while west-side roofs were not damaged (f0).
Below: An enlarged view of a 9"X9" vertical photo taken by Continental Aerial Survey on 8/27/92.

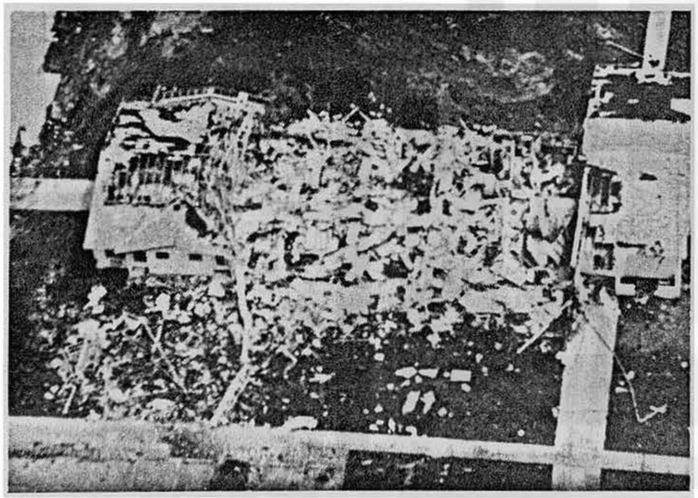

Left: Aerial photo of a tie-beam (see map) blown off toward the west. Fujita photo 1245 EDT 9/14/92.
Right: Ground view of the tie-beam reinforced with one-inch steel rods. Fujita photo 1649 EDT 9/15/92.

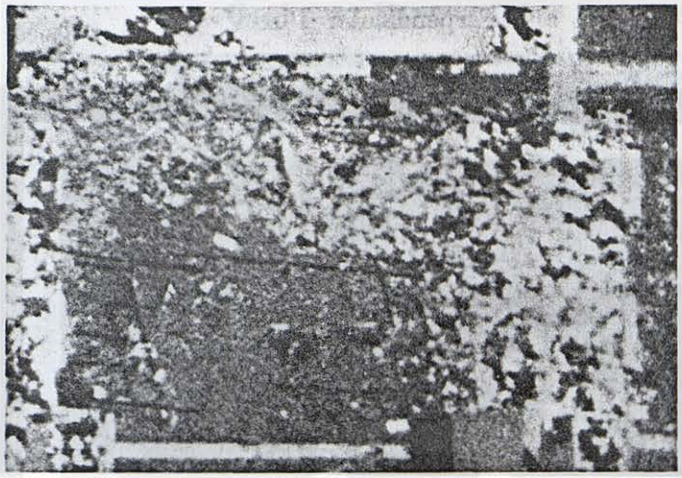

Left: Tie-beams at Pine Woods Villa (see map) blown apart by a mini-swirl. Continental Aerial Survey photo taken on 8/27/92. **Right:** Ground view of the tie-beams. Fujita photo 1109 EDT 9/9/92.

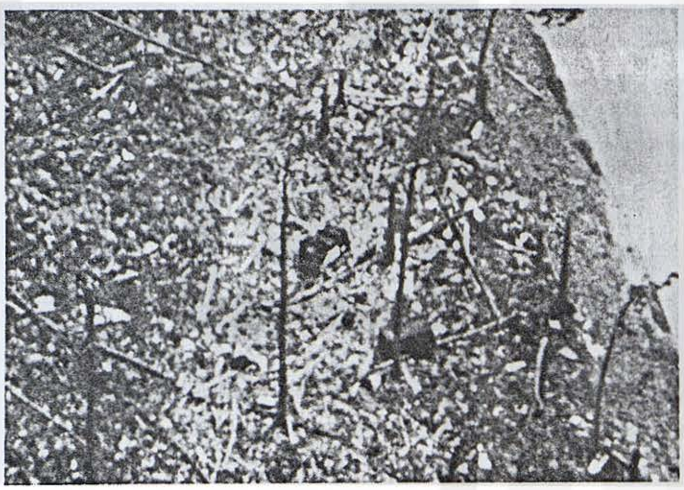

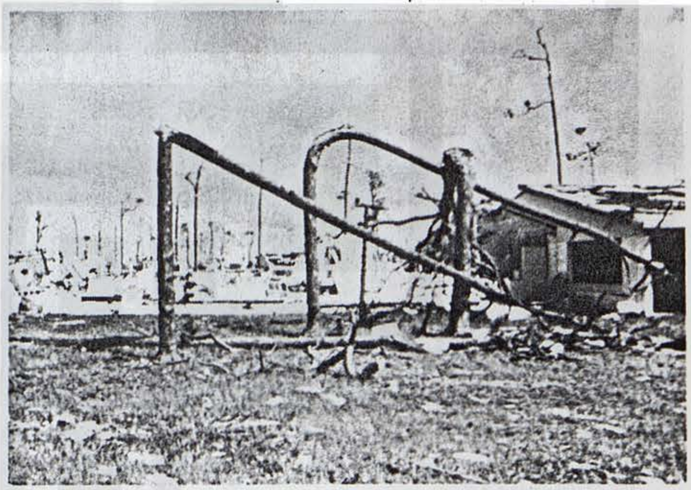

Left: A dumpster found inside the high-speed debris (see map). Some trees in this photo were blown down by both first and second winds. Fujita photo 1234 EDT 9/14/92. **Right:** Bi-directional tree damage seen near the dumpster site. Fujita photo 1109 EDT 9/9/92.

Left: An impact hole (see map) created by a falling tie-beam. Fujita photo 1245 EDT 9/14/92. A piece of flying plywood cut through the trunk of the tall pine tree shown at the lower left of the picture. **Center:** Drs. Robert Sheets and Peter Black examining the tree trunk. **Right:** A close-up view of the deep cut. Fujita photos 1057 EDT 9/9/92.

Condos at Naranja Lakes in Wind-parallel and Perpendicular Directions

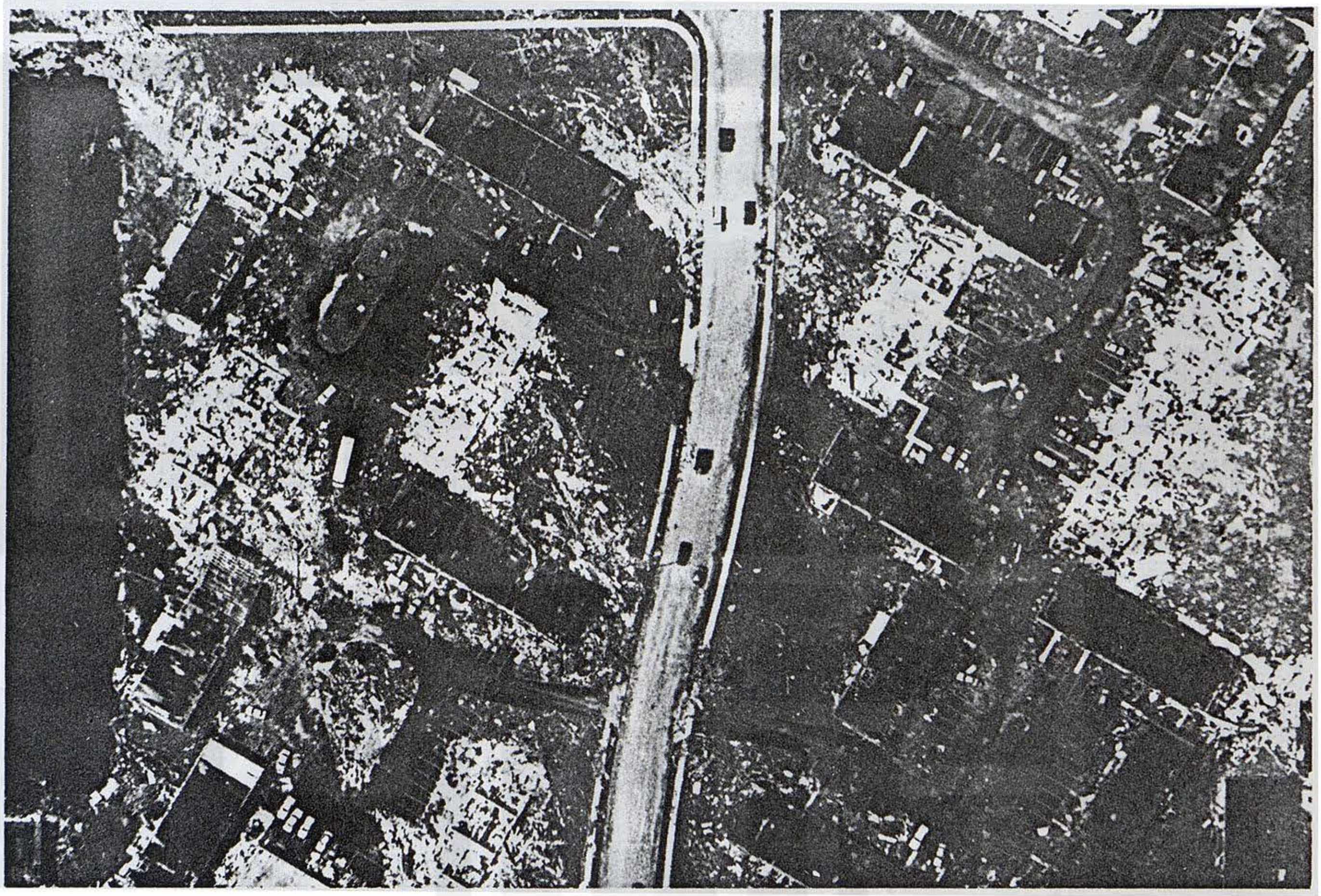

Center of Andrew's eye passed directly over Naranja Lakes, resulting in a 180° shift of the first wind from NNW into the second wind from SSE. Many buildings oriented WSW-ENE (wind-perpendicular) direction received the f3 damage while those in the NNW-SSE (wind-parallel) direction were spared. Enlargement of a Continental Aerial Survey photo taken on 8/26/92.

Left: A Naranja Lakes condo oriented in the wind-perpendicular (broadside) direction. The roof was lifted into a vertical position and dropped upside-down after a 180° rotation. Connected and broken tie-beams weighing one ton per 20 ft are visible on the downwind side. Fujita photo 1253 EDT 9/14/92. **Right:** Mobile homes at Naranja Lake oriented by luck in the wind-parallel (streamline) direction. Fujita photo 0906 EDT 9/8/92.

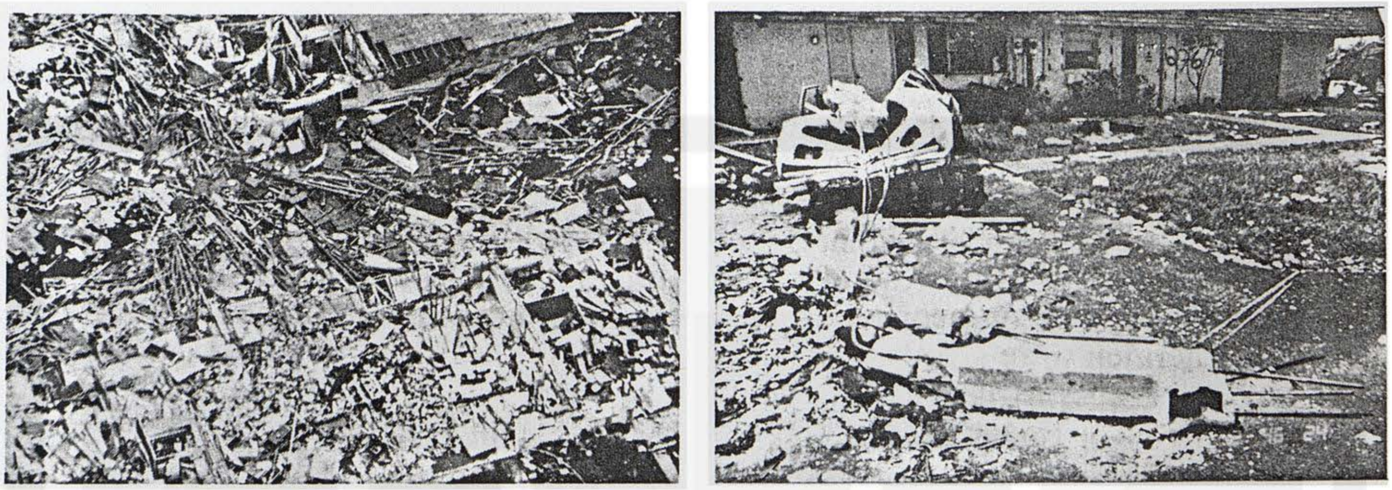

Left: An f3 damage of Naranja Lakes condo caused by a mini-swirl that formed inside the second wind. Fujita photo 1253 EDT 9/14/92. **Right:** Pieces of a connected tie-beam which flew 150 feet (45m) from a Naranja Lakes condo in the second wind. Fujita photo 1246 EDT 9/10/92.

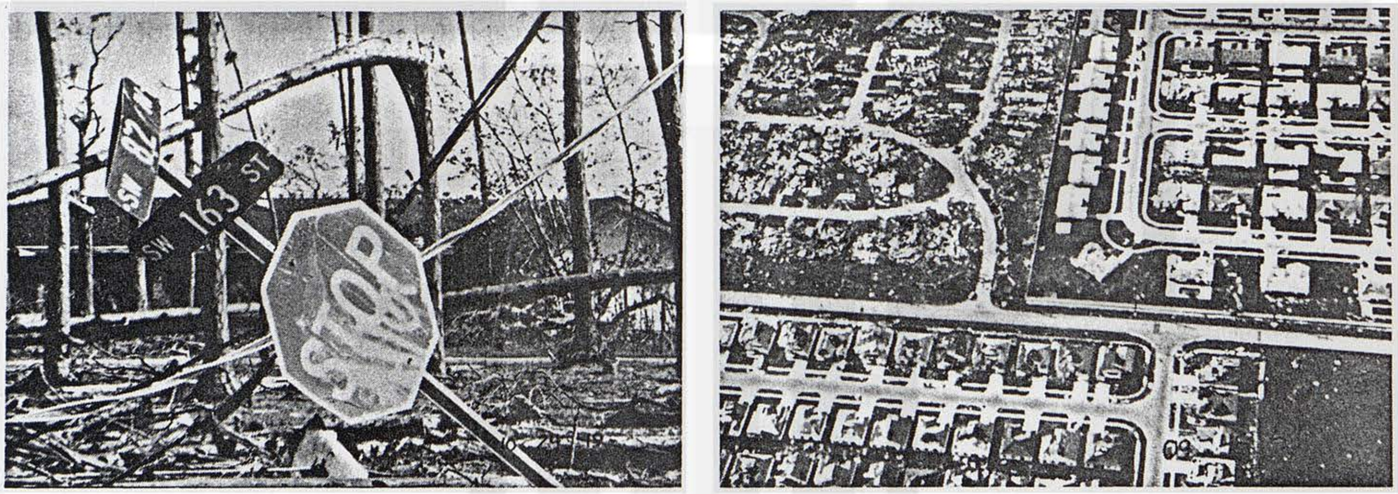

Left: A confusing stop sign at 82 Ave and 163 St SW in Cutler located near the north edge of the Tamiami Swath. Fujita photo 1024 EDT 9/16/92. **Right:** Triple junction of f-scale damages. An f4 damage at a trailer park (upper left), f2 at the lower-left subdivision, and f0 to f2 at the upper right subdivision. Relatively uniform peak winds (F-scale winds) expected at the junction caused a wide range of f-scale damages between f0 and f4. Fujita photos 0945 EDT 9/8/92. **Note that the Fujita Scales, now applied to both tornadoes and hurricanes, refer to the Fujita Wind Speed scale (F scale) and Damage scale (f scale),** because an F-scale wind would cause different f-scale damages to different types of structures. See examples.

FOLDING COLOR MAP OF HURRICANE ANDREW

This issue of STORM DATA includes the following four maps printed in multiple colors on a 15" x 21" folding sheet. These maps are:

1. **Overall Damage Map of Andrew**
2. **Map of the first wind**
3. **Map of the second wind**
4. **Estimated winds at 10,000 ft altitude**

The research presented in this contributed paper by T. Theodore Fujita, of the University of Chicago, has been sponsored by NASA under Grant NAG8-886 and ONR under Grant N00014-91-J1136.

Damage Map of Hurricane Andrew on August 24, 1992

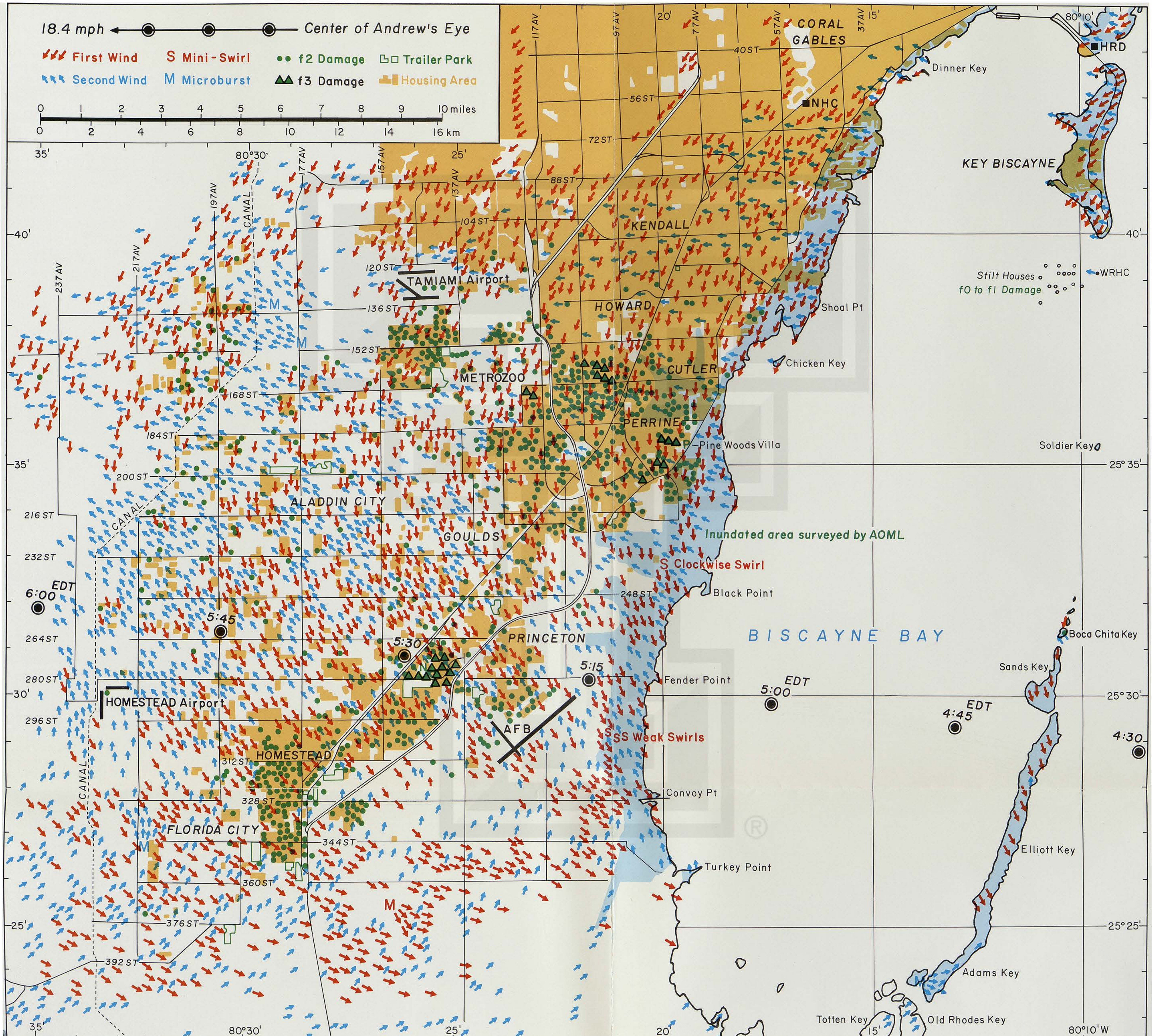

Section Five

Mini-swirls at Naranja Lakes

Naranja Lakes subdivision is located four miles northwest of Homestead AFB and six miles west of the Biscayne Bay shoreline. The center of Andrew passed from east to west directly over the subdivision between 5:25 and 5:30 a.m. EDT at an 18 mph translational speed (refer to color map in Section 4).

Due to the passage of the eye center over the subdivision, the first wind from 325° changed into the second wind from 155°. The 170° cyclonic shift took place within 20 to 30 minutes (see Figure 3.4).

Detailed aerial photographs revealed that six (6) mini-swirls (1-a through 1-f in Figure 5.1) damaged the Naranja Lakes area during the first wind. All of the mini-swirls embedded inside the first wind traveled from northwest to southeast. Most of the mini-swirls rotated anticyclonically, inducing the strongest total wind on the northeast side of their swaths which were 200 to 400 feet wide and 500 to 2,000 feet long.

Nine (9) mini-swirls occurred at Naranja Lakes during the second wind, all of which moved from southeast to northwest (see Figure 5.2). Six (6) rotated cyclonically, while three (3) others rotated anticyclonically. As expected, the 6 cyclonic mini-swirls induced the maximum wind on the northwest side of their swaths, and the anticyclonic mini-swirls induced the maximum wind on the southeast side of their swaths.

In all, fifteen (15) mini-swirls were confirmed inside the Naranja Lakes subdivision. 1-a through 1-f occurred during the first wind and 2-a through 2-i, during the second. It is seen in Figure 5.3 that the first-wind and second-wind swirls are co-located. "Is this accidental?" Close examination reveals that the initial points of the second-wind swirls are often located inside the damage areas of the first-wind swirls. This means that these structures (condos), already damaged or weakened by first-wind swirls, became easy targets for destruction by the second-wind swirls. In fact, some condos received dual damage caused by both first- and second-wind swirls.

Most of the damaged condos lost their roofs which were lifted and turned upside-down. Naturally, the overturning moment is largest in the wind-parallel direction and smallest in the wind-perpendicular direction. Consequently, wind-perpendicular condos received the worst damage. The variation of damage is more or less sinusoidal (see Figure 5.4), with the maximum occurring at 52° and the minimum at 135°. Wind-perpendicular orientations during the first wind from 325° and the second wind from 155° are 55° and 65°, respectively. This means that condos in 55° and 65° orientations could receive severe damage. These orientations are within 15° of the 52° orientation shown in Figure 5.4. The difference could be the result of the mini-swirl rotation and the predominant orientation of condos at 0° and 90°.

The index map/photo in Figure 5.24 shows the eight (8) specific locations enlarged and presented in Figures 5.5 through 5.23 which include Fujita's color photos and analyses. These photos are explained by the captions accompanying each.

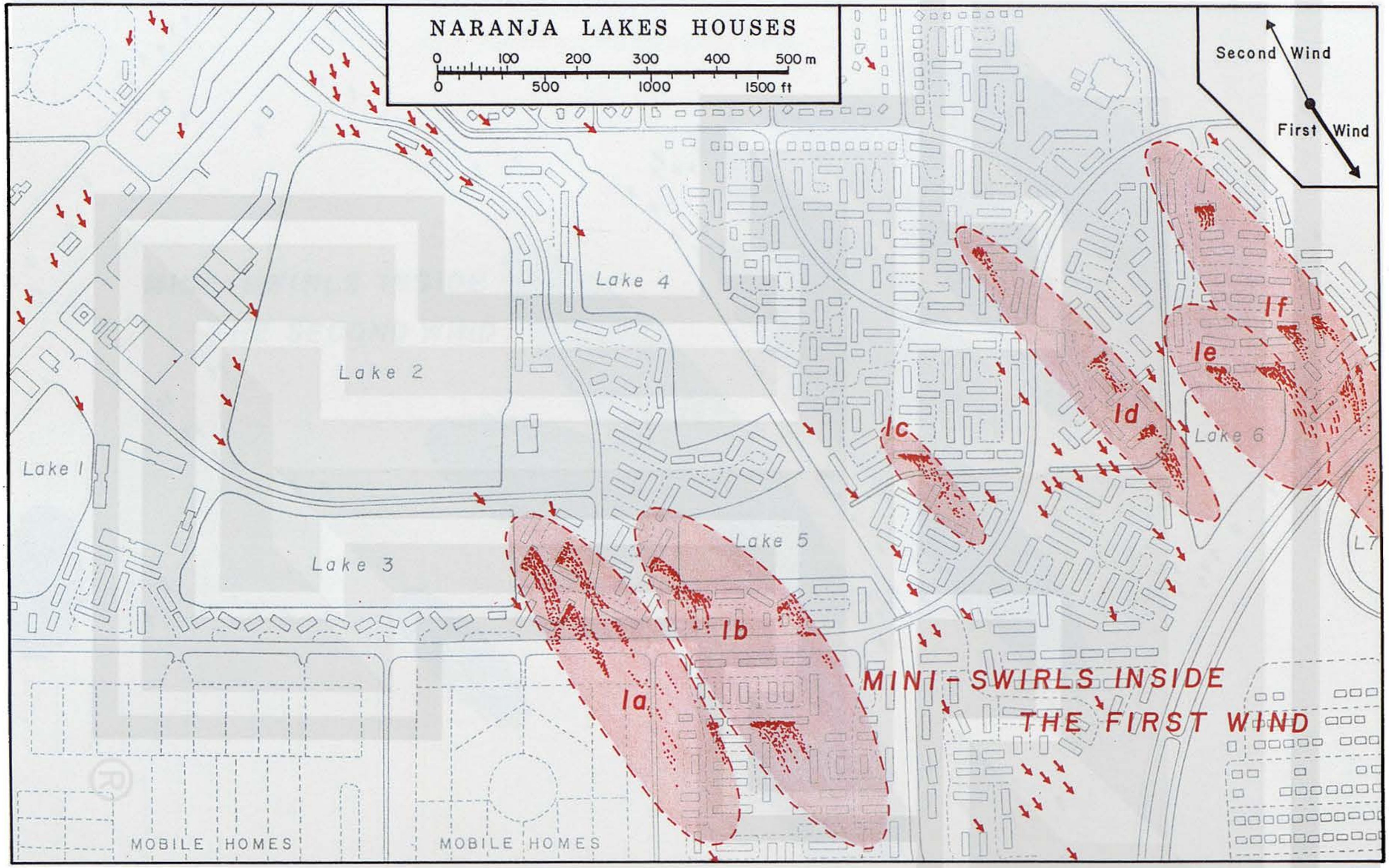

Fig. 5.1 Six swaths of the mini-swirls in the Naranja Lakes area. All of the swirls rotated anticyclonically.

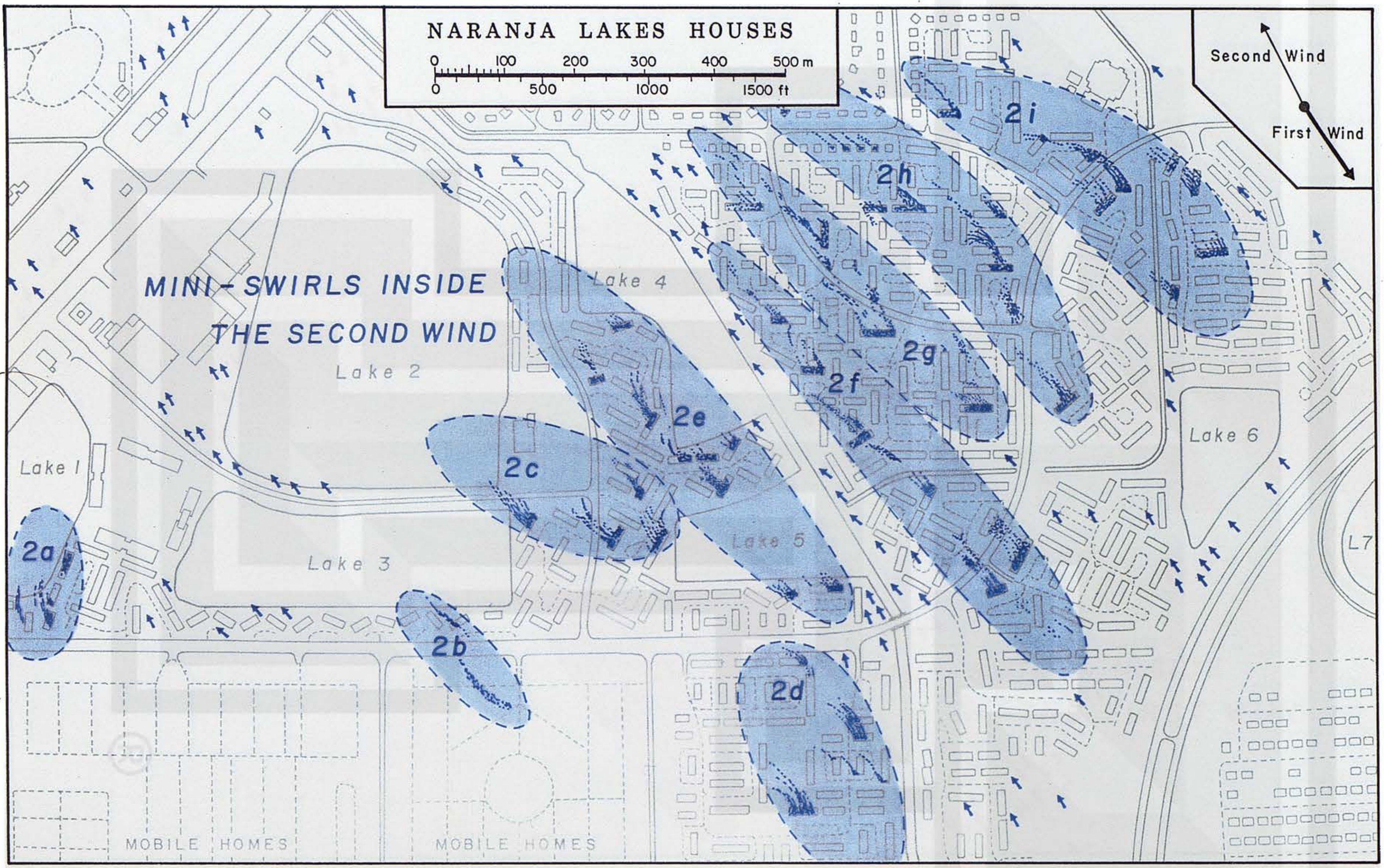

Fig. 5.2 Six (6) cyclonic mini-swirls (2d, 2f-2i) and three (3) anticyclonic mini-swirls embedded inside the second wind blowing from the southeast.

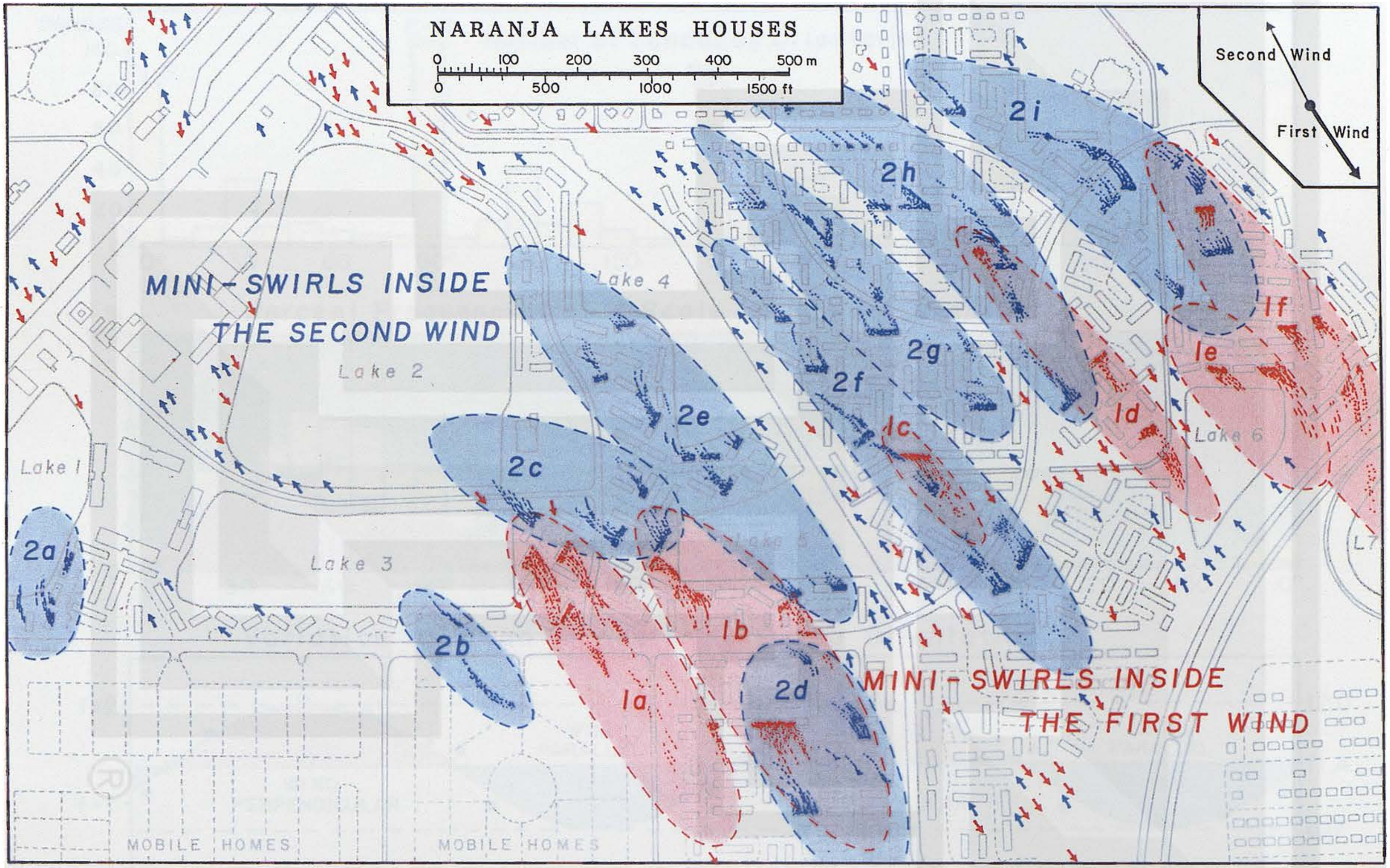

Fig. 5.3 Swaths of the 15 mini-swirls induced by Andrew at Naranja Lakes. Note that the damage of second-wind mini-swirls 2c, 2h and 2I occurred inside the damage areas of first-wind mini-swirls.

f - Scale Distribution of Naranja Lakes Condos

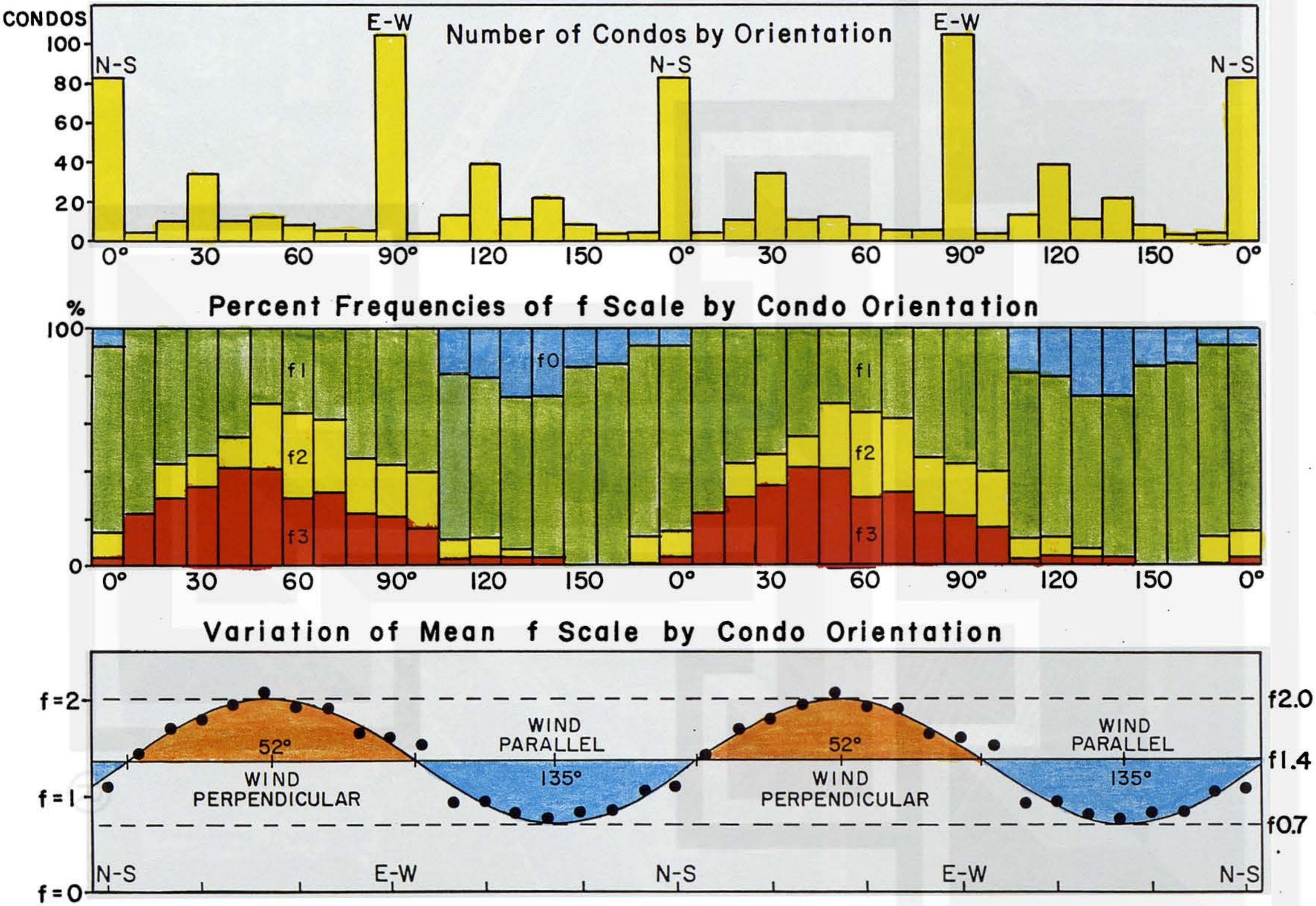

Fig. 5.4 Frequencies of the F-scale damage in relation to the wind-parallel orientation of Naranja Lakes condos. The orientation denotes the azimuth angle of the long axis of each condo.

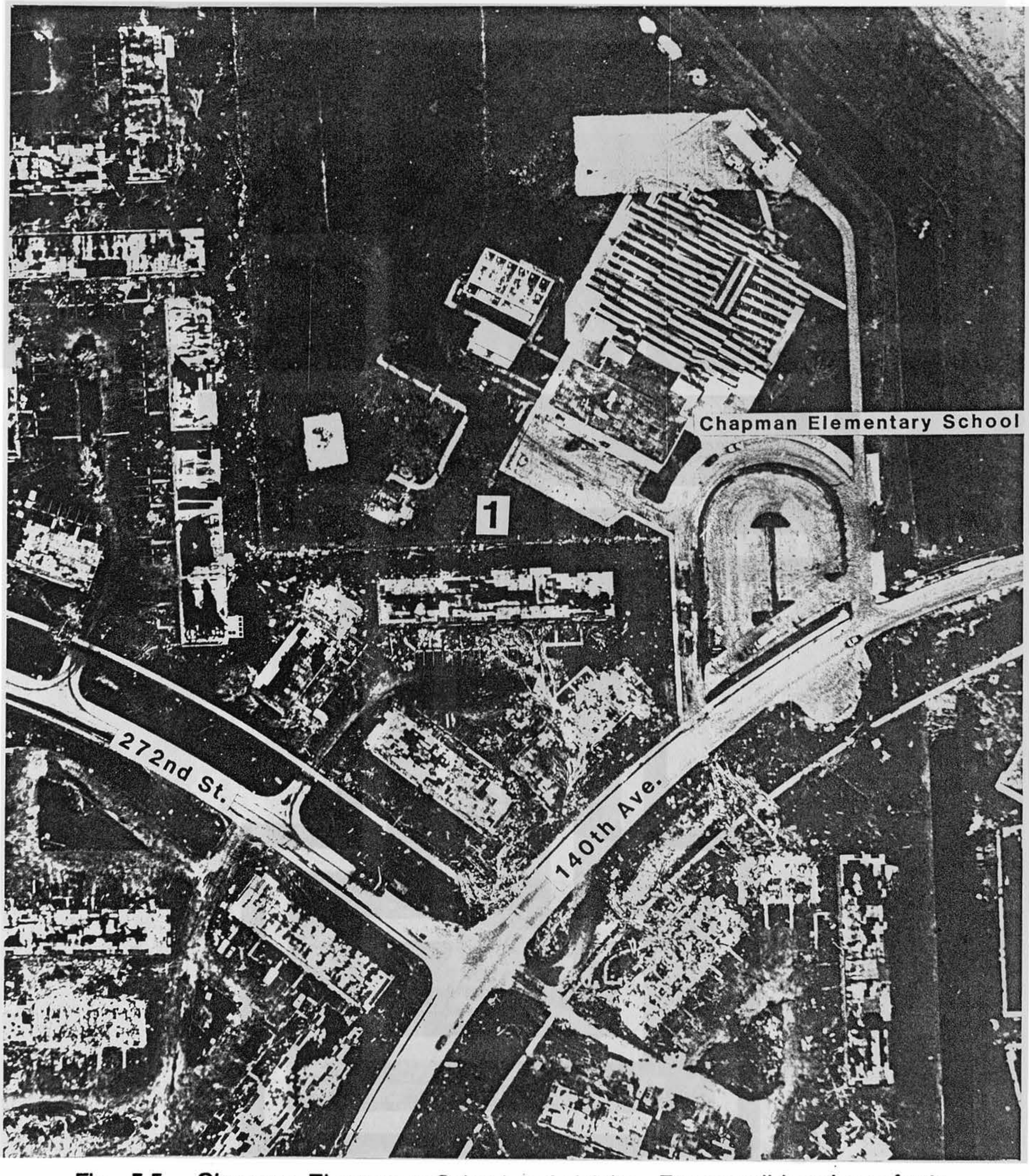

Fig. 5.5 Chapman Elementary School and vicinity. For overall location refer to the index map in Figure 5.24.

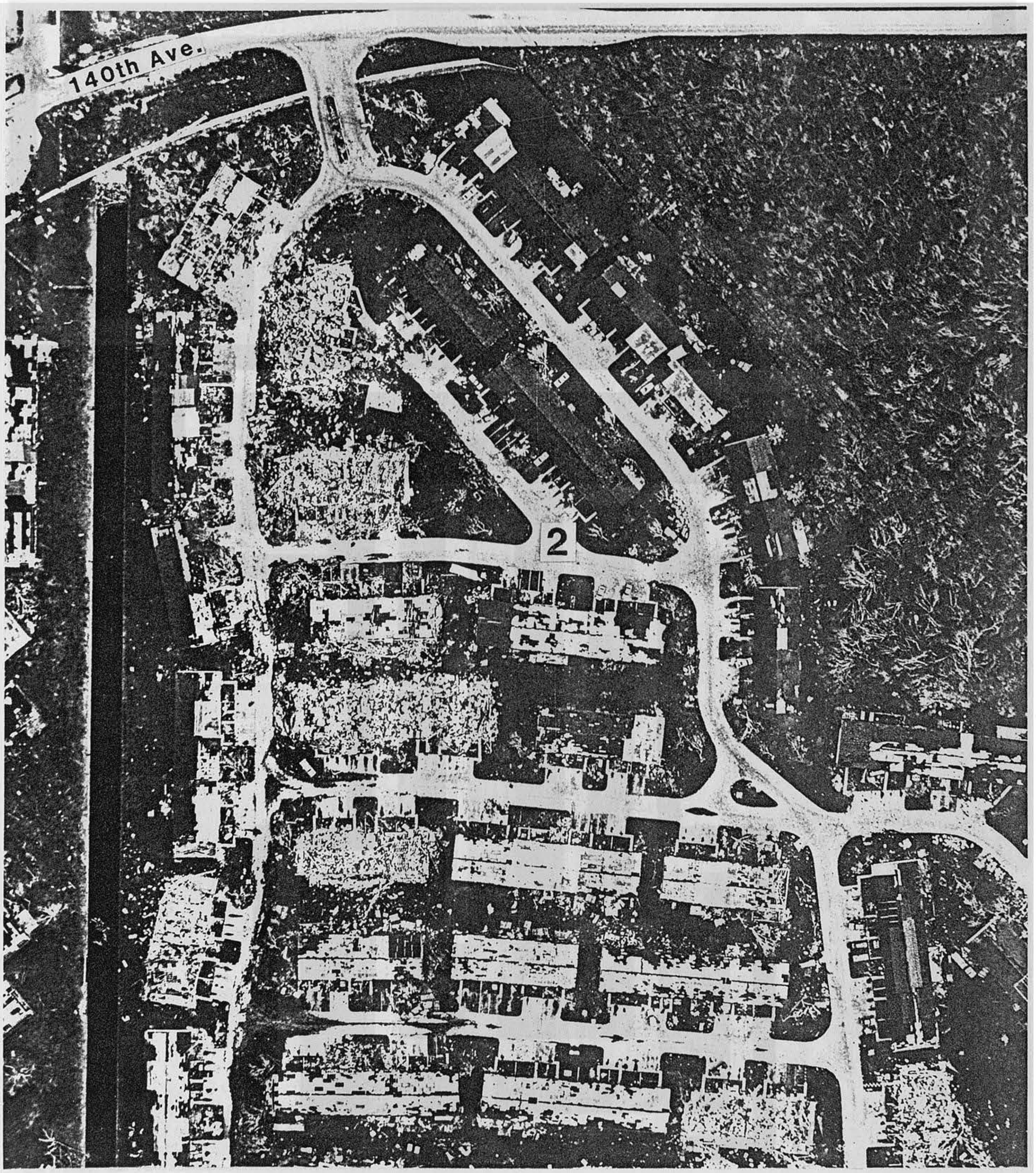

Fig. 5.6 A residential area southeast of Chapman Elementary School. Effects of both first and second winds are visible.

Fig. 5.7 **A.** Southern half of a condo blown toward the northwest by the second wind. **B.** Severe damage of twin condos caused by a cyclonic mini-swirl that moved north-northwest. **C.** Condos damaged by the first swirl.

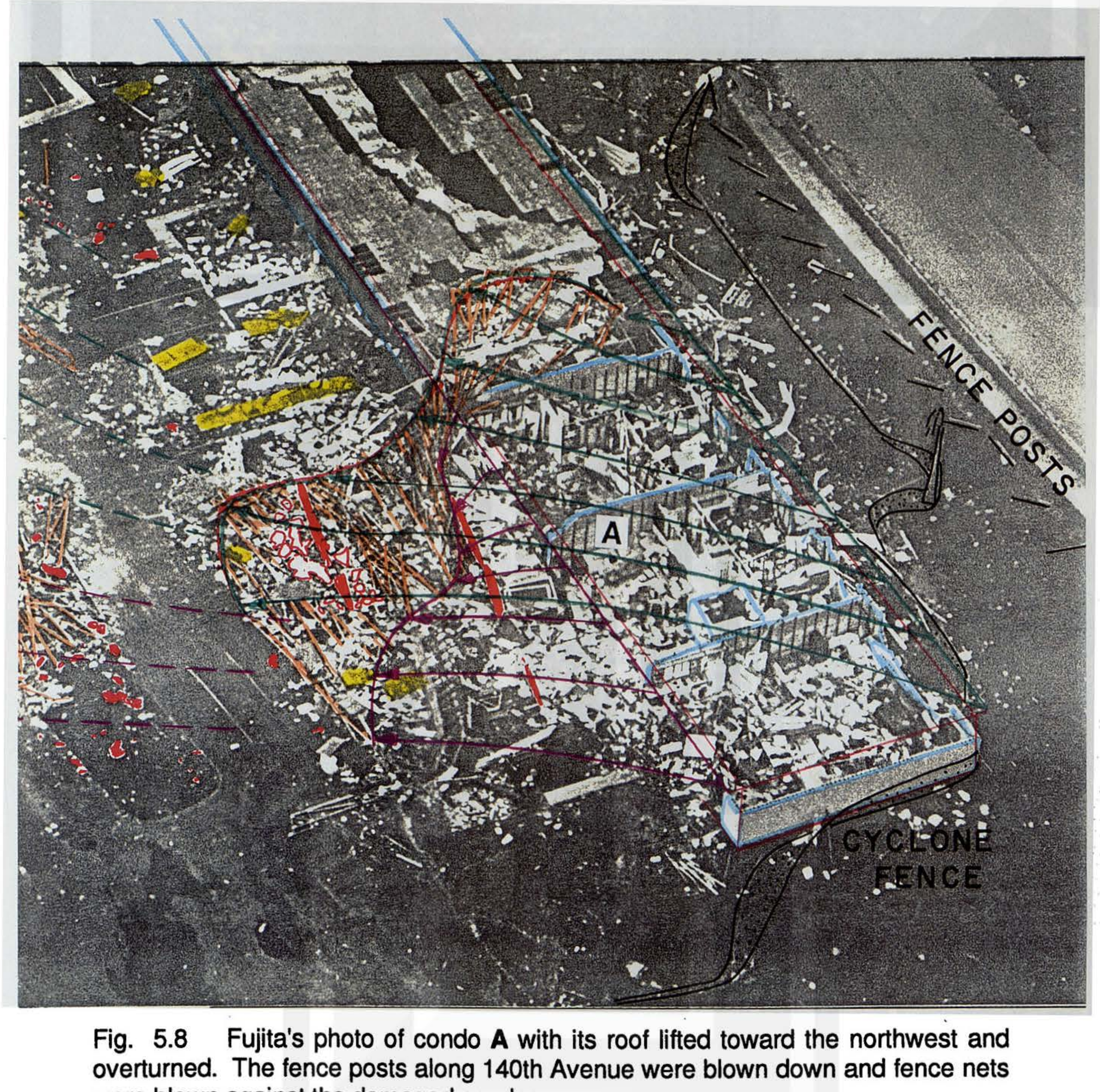

Fig. 5.8 Fujita's photo of condo **A** with its roof lifted toward the northwest and overturned. The fence posts along 140th Avenue were blown down and fence nets were blown against the damaged condos.

Fig. 5.9 **B.** Twin condos west of 140th Avenue. The northern condo was unroofed first. Then the roof of the southern condo landed on top of it in an upside-down position. The center of a mini-swirl moved over the condos in a north-northwest direction.

Fig. 5.10 Fujita's aerial photo of the twin condos. Two tie beams (colored in red), one on the north side and the other on the south side, landed in an upside-down position and broke.

B

Fig. 5.11 Fujita's color picture showing the severe damage (estimated F4) caused by a cyclonic mini-swirl which moved toward the north-northwest.

Fig. 5.12 **C.** Twin condos damaged by the first wind / first swirl. **D.** The worst damage to a condo, next to a narrow canal. It is seen that a condo to the south was blown off toward **D.**

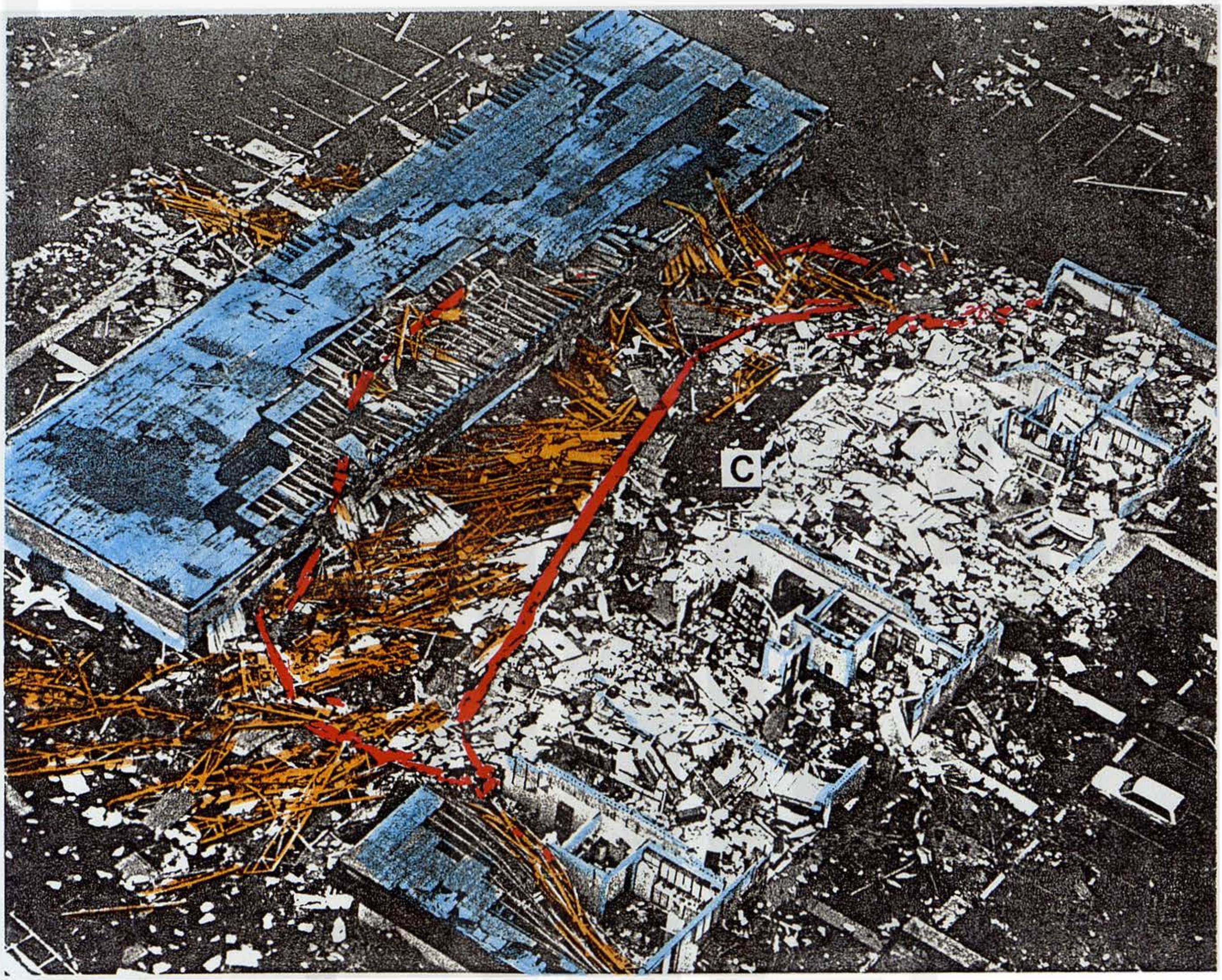

Fig. 5.13 The final position of the north and south tie beams of condo **C**. It is likely that the roof with the tie beams was lifted front side first. Then the roof flipped over and crashed onto the roof of the north condo. The south tie beam was broken into pieces upon hitting the north condo's roof.

C

Fig. 5.14 Fujita's aerial photo showing the detailed pattern of damage.

Fig. 5.15 Condo **D** damaged severely by an anticyclonic mini-swirl which moved from north to south crushing the condo and throwing its concrete debris into the canal to the south.

D

Fig. 5.16 Fujita's color photo showing the detailed damage of condo **D**. A mini-swirl in the first wind destroyed the western half of the condo (left to right), pushing off the front (north side) tie beam across the canal to the south of the condo.

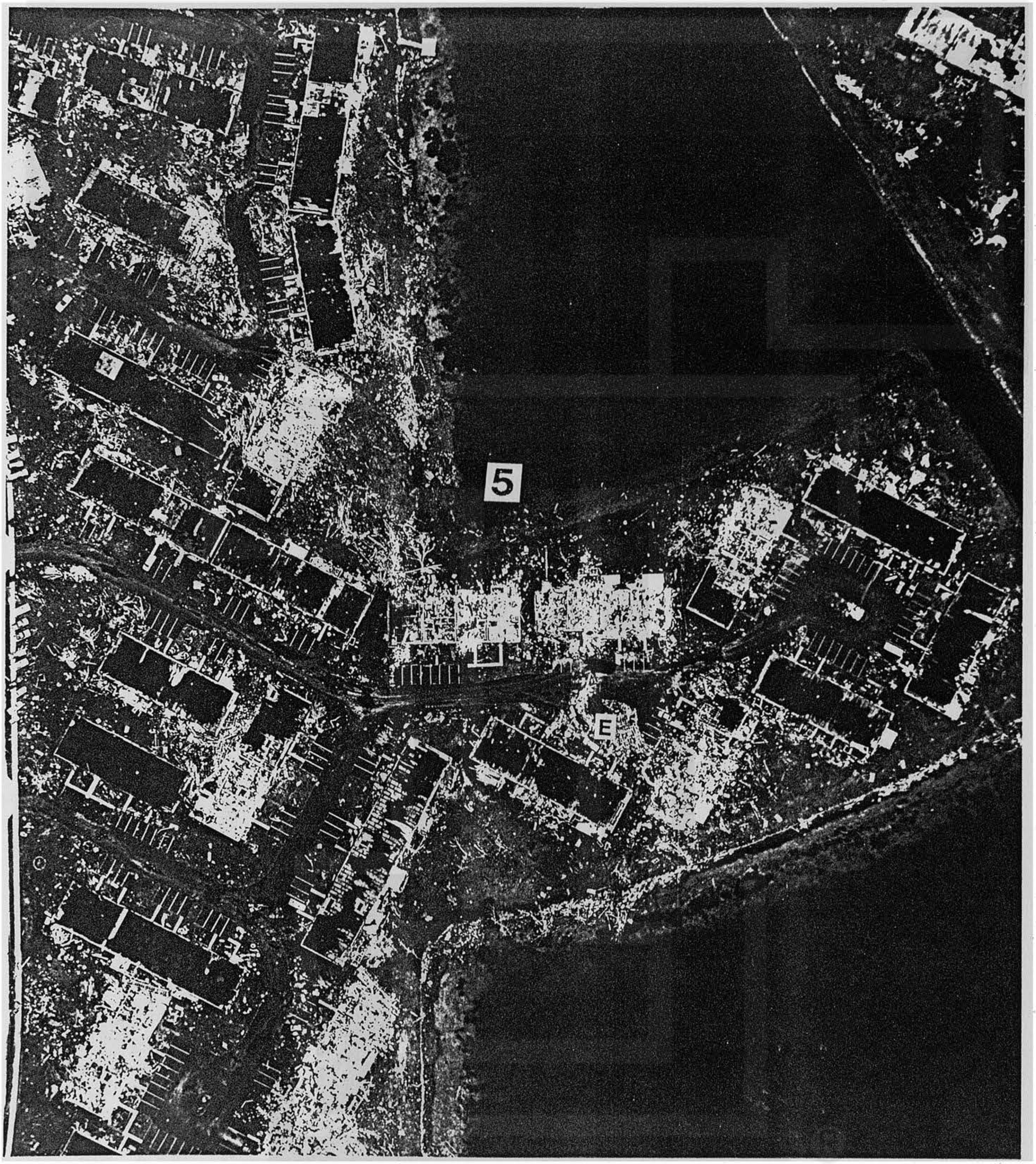

Fig. 5.17 Overall area of condo **E** which was unroofed and pushed toward the northwest. Its roof with tie beam crash-landed at **E**.

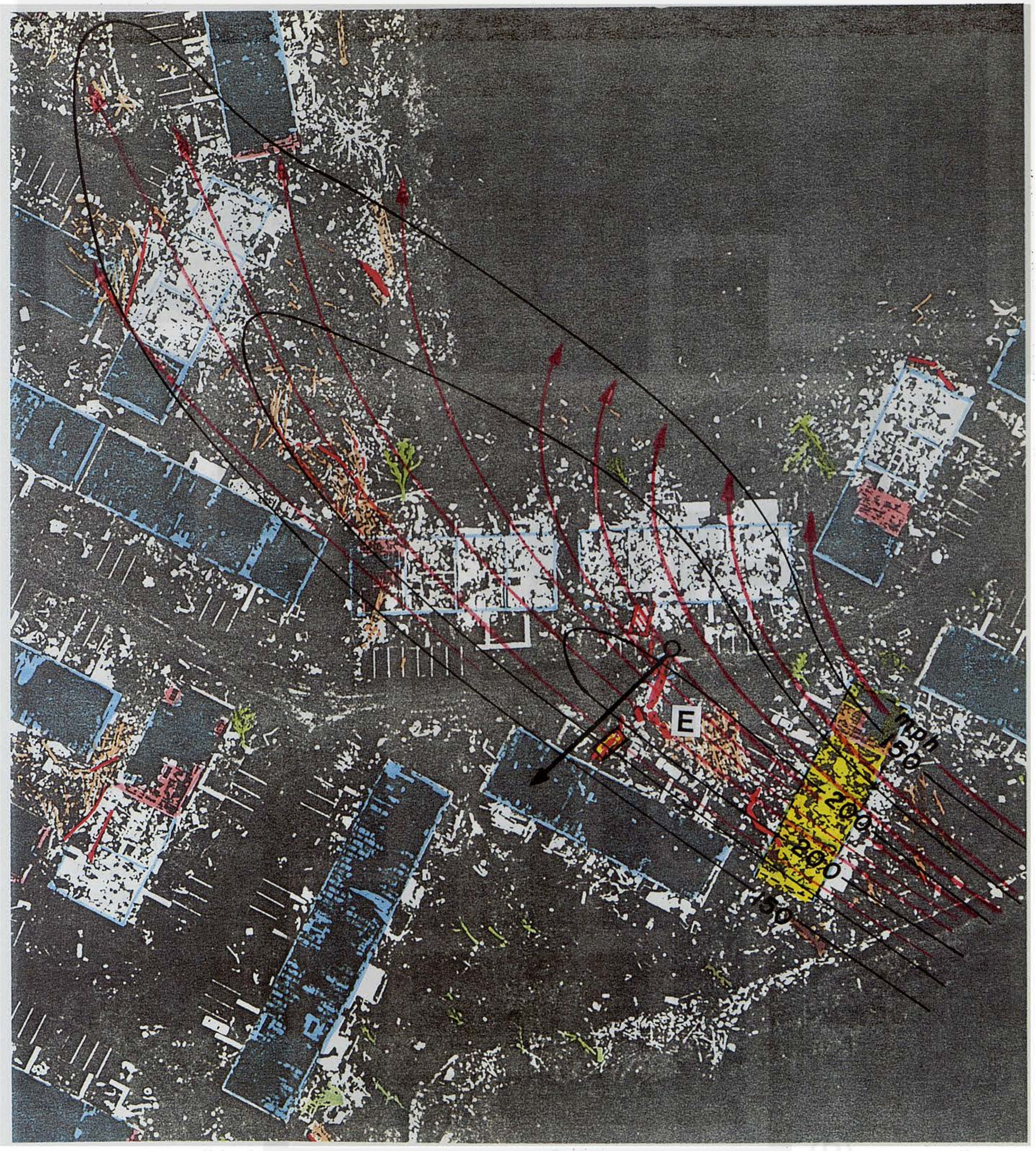

Fig. 5.18 Schematic streamlines and estimated windspeed of 200 mph which caused the broken-up tie beam to be thrown 250 feet onto a parked car (Figure 5.19).

E

Fig. 5.19 Pieces of the tie beam blown onto a parked car in a lot downwind from condo **E**. A wind-parallel condo seen in the background was particularly undamaged.

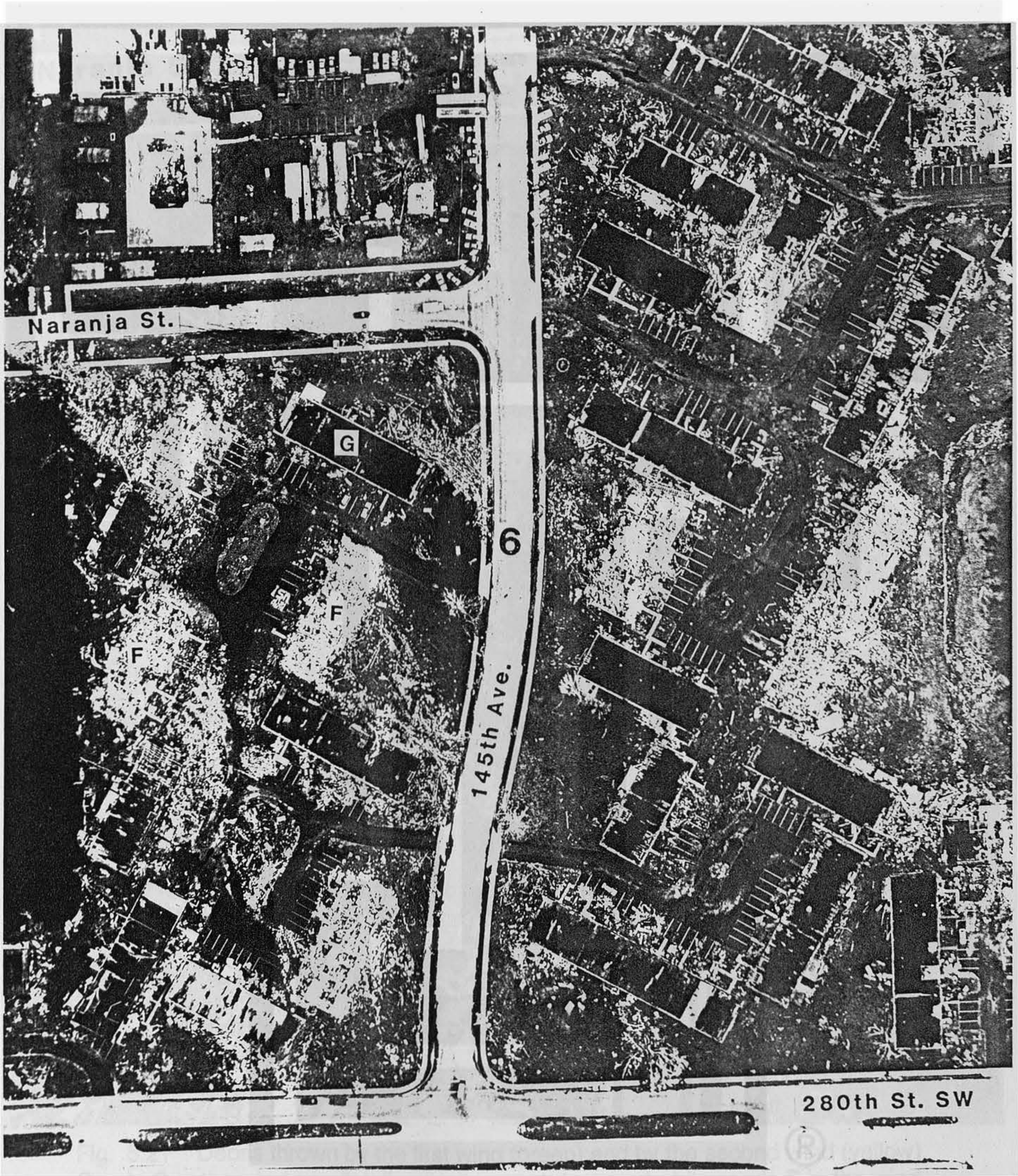

Fig. 5.20 An overall view of the damaged condos oriented in the 120° (wind parallel) and 30° (wind perpendicular) directions.

Fig. 5.21 Debris thrown by the first wind (green) and by the second wind (yellow). Condo **G** in the wind-parallel direction was not damaged while condo **F** in the wind-perpendicular direction was damaged severely.

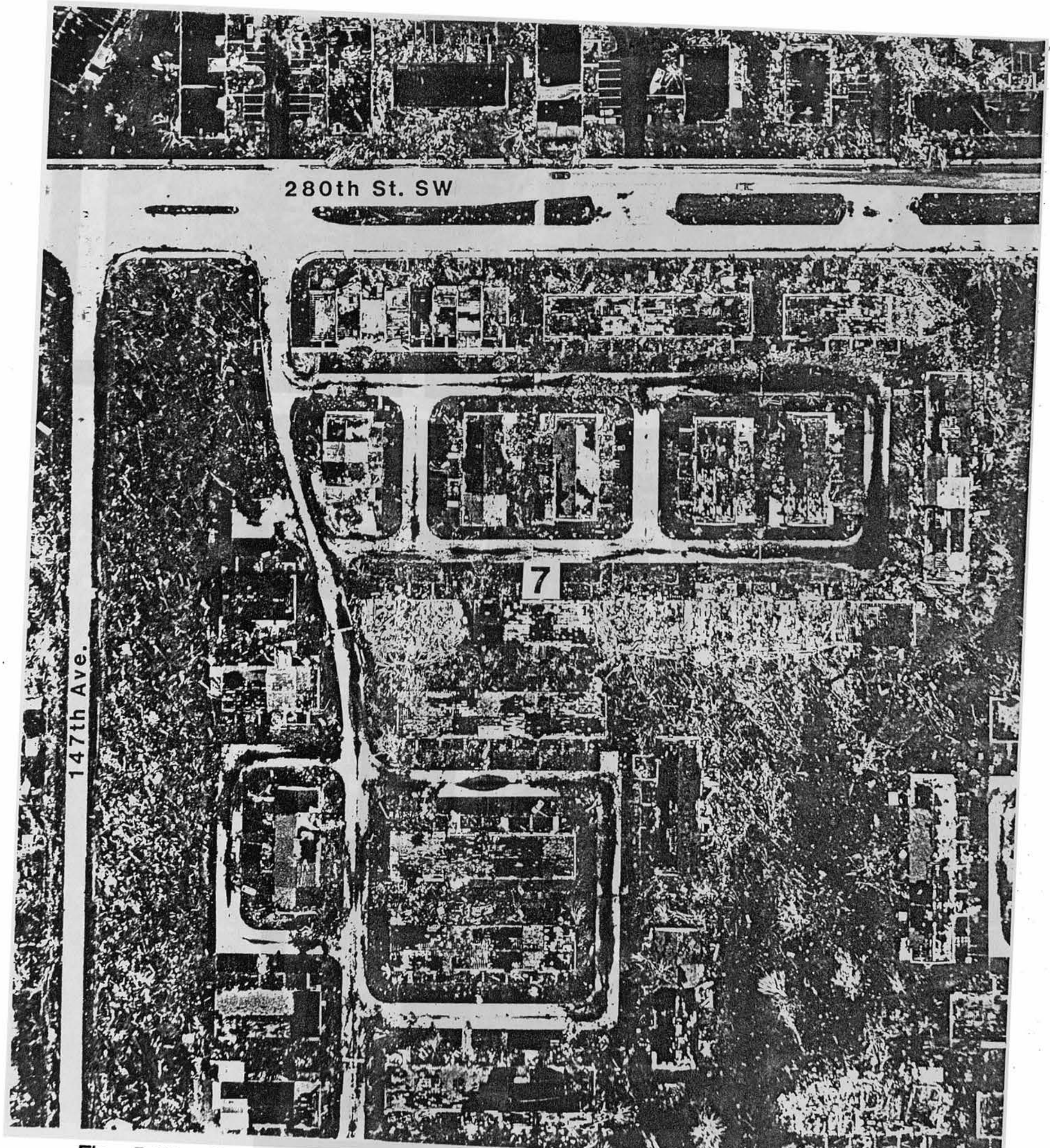

Fig. 5.22 Wind-parallel condos south of 280th Street SW damaged by the first wind from north-northwest.

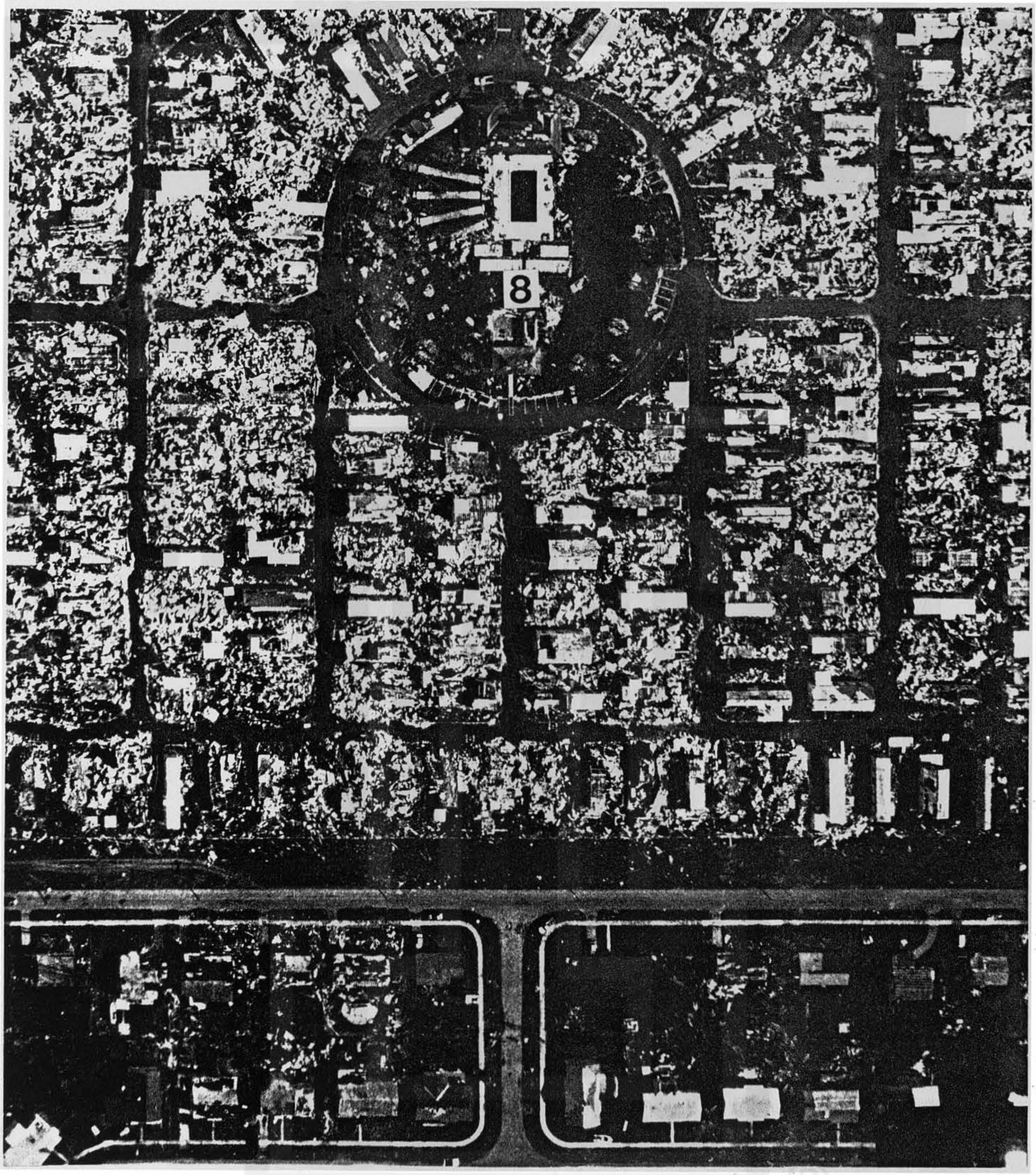

Fig. 5.23 Unexplainable damage of the mobile-home park south of 280th Street SW. Some mobile homes were untouched by the high winds. Why?

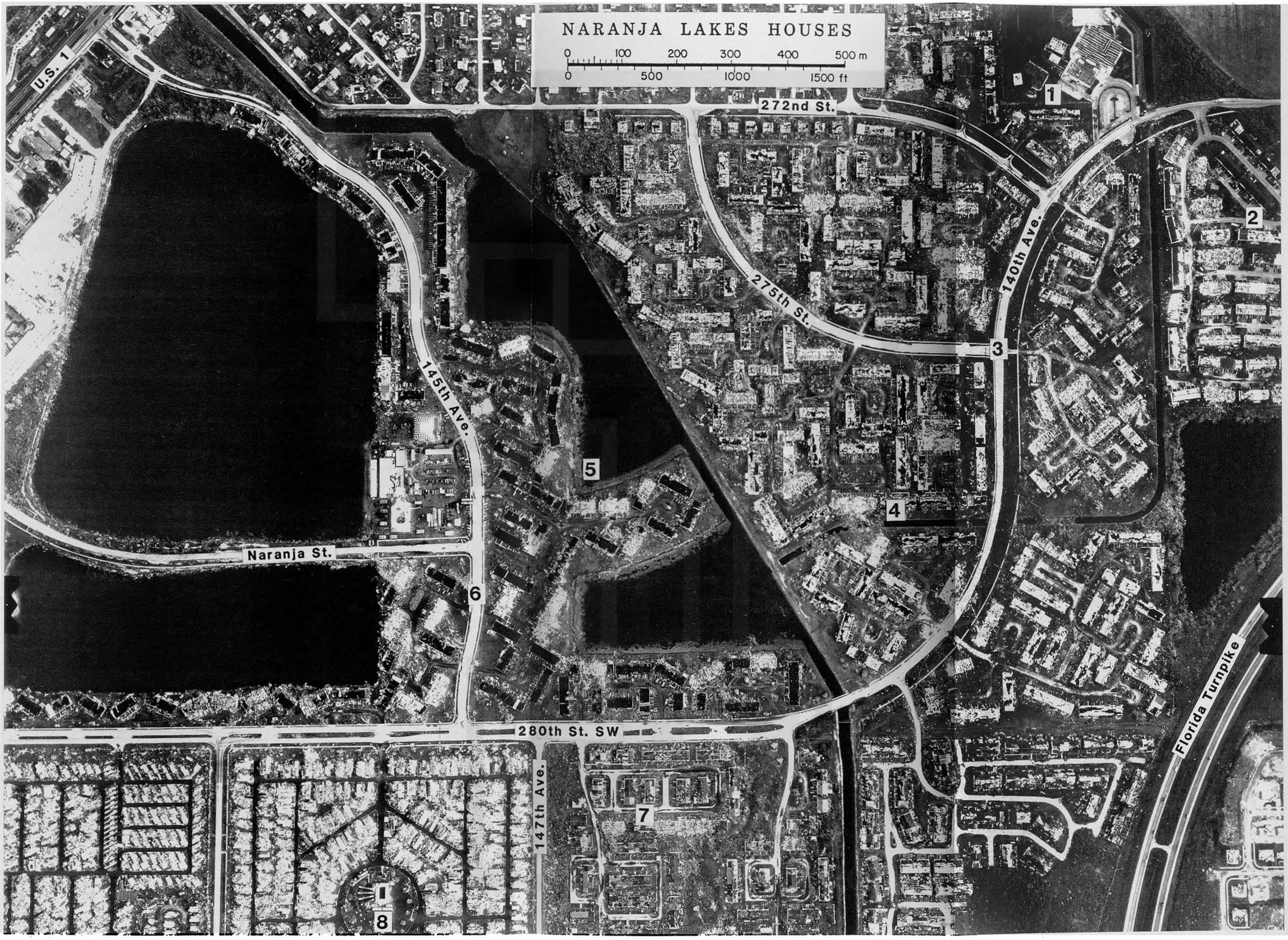

Fig. 5.24 An index map of the Naranja Lakes subdivision, consisting mainly of single-story condos. Areas **1** through **8** were enlarged.

Section Six

Mini-swirls at Pine Woods Villa

Pine Woods Villa, located at 87th Avenue and 188th Street SW in Perrine, 15 miles southwest of Downtown Miami, was severly damaged by Hurricane Andrew. Most of the angles between the wind direction and condo axes were 45°. Amazingly, however, the estimated maximum winds are 200 mph. Roofs were blown off and supporting tie beams were thrown a considerable distance. Some tie beams were stripped from the structure while others flew through the air. One of them left behind a sharp cut as it landed on a roof.

It was concluded that six (6) mini-swirls, all rotating anticyclonically, occurred inside the first wind. Their rotational speeds were estimated at 50 to 70 mph and their translational speeds, 120 to 130 mph. The total speed excluding vertical motion could reach 170 to 200 mph.

Along with the Naranja Lakes mini-swirls, the Pine Woods Villa mini-swirls induced damaging winds that exceeded significantly the so-called "sustained wind". At this magnitude of wind force, destruction will be completed in less than 10 seconds, far shorter than the one-minute period of sustained winds.

An index map/photo, identifying specific locations of Pine Woods Villa, is presented in Figure 6.10. Enlarged photos and analyses of these sites are presented in Figures 6.1 through 6.9 along with explanitory captions.

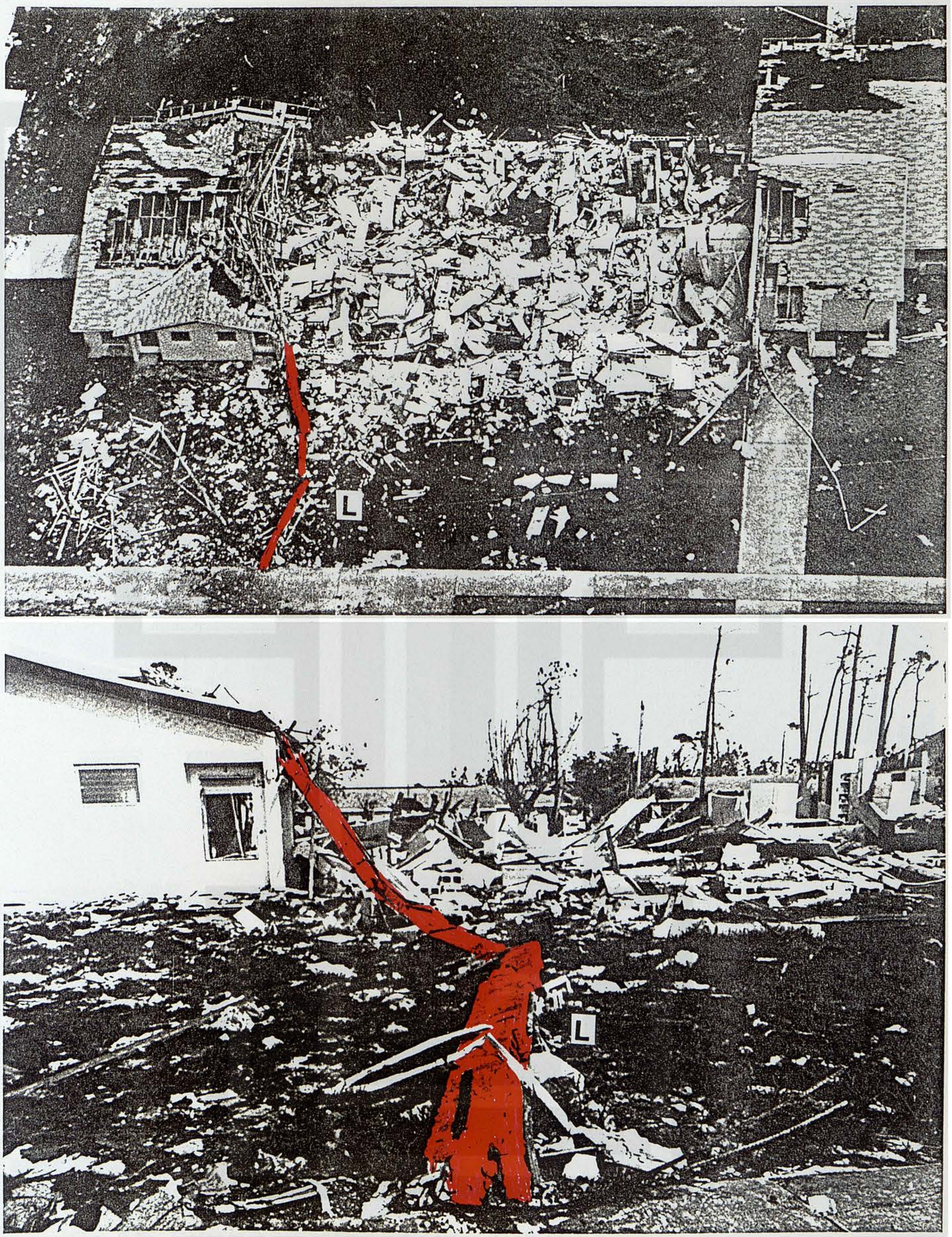

Fig. 6.1 A tie beam from condo **L** photographed from the air and on the ground by Fujita. A mini-swirl in the first wind caused this damage (see index map, Figure 6.10).

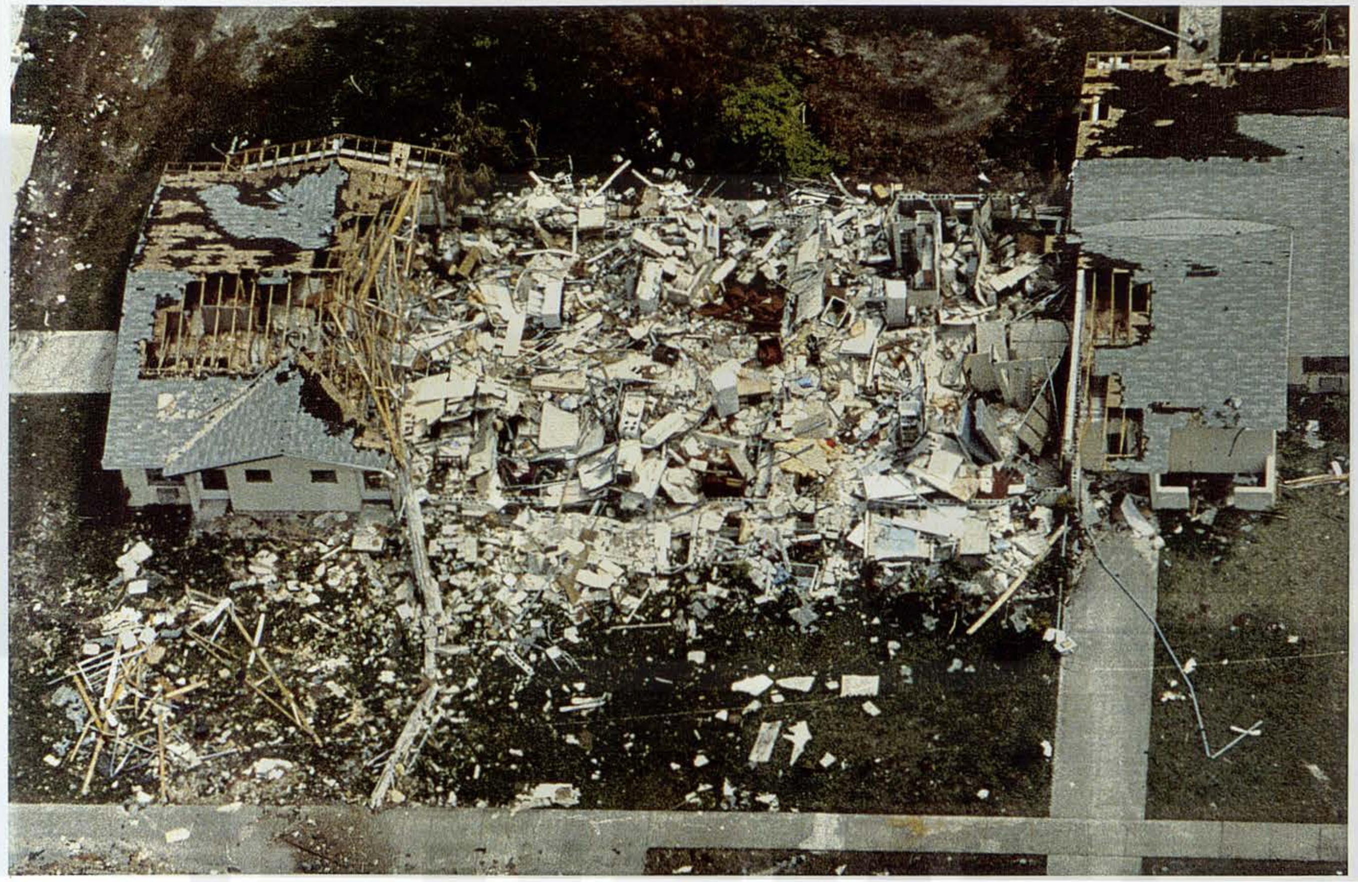

Fig. 6.2 Color pictures of Figure 6.1 taken by Fujita.

Fig. 6.3 Swirling patterns left behind by a mini-swirl in the first wind. Red streaks denote the streamlines of the swirl.

M

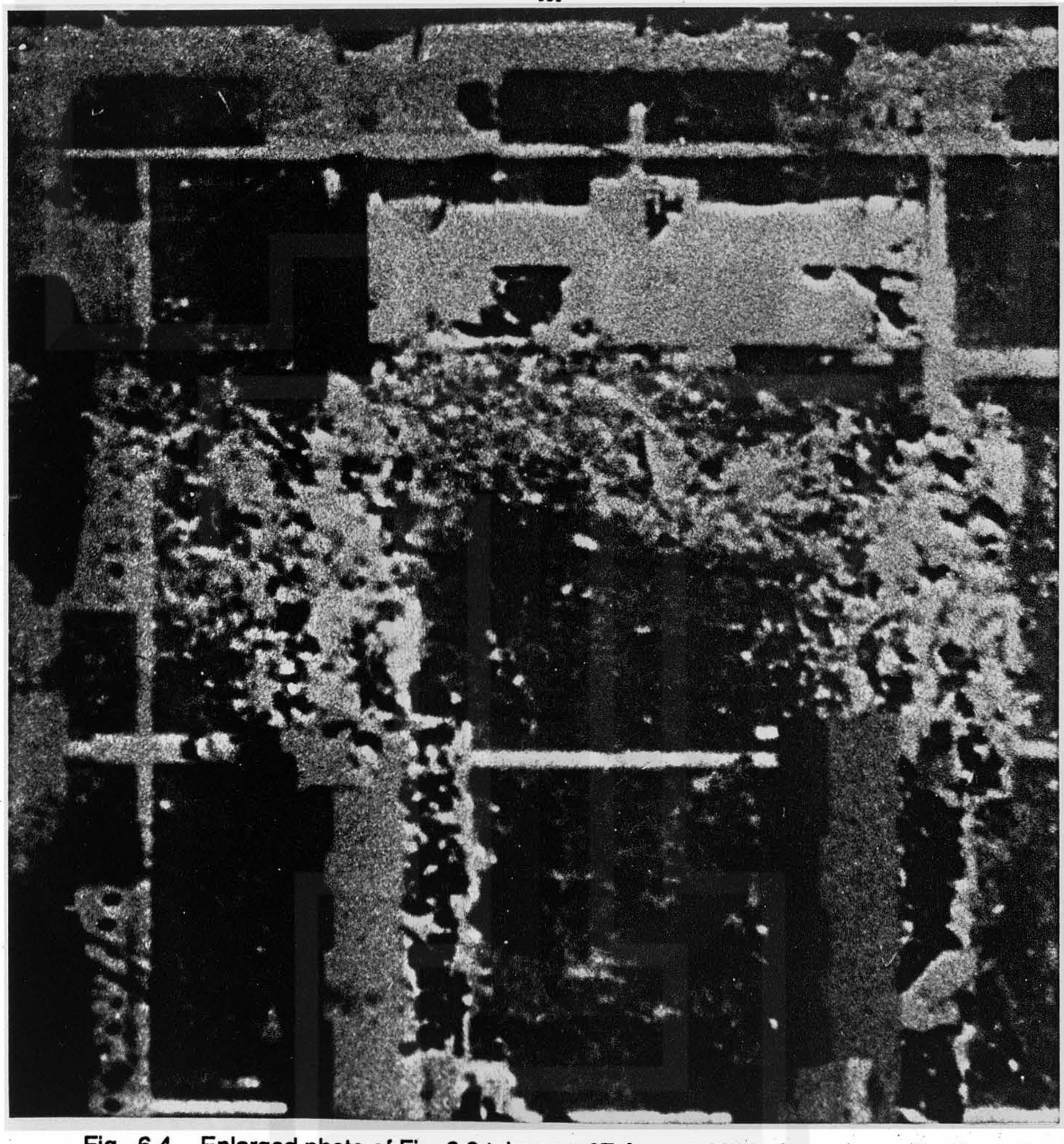

Fig. 6.4 Enlarged photo of Fig. 6.3 taken on 27 August 1992, three days after the storm, by Continental Aerial Survey.

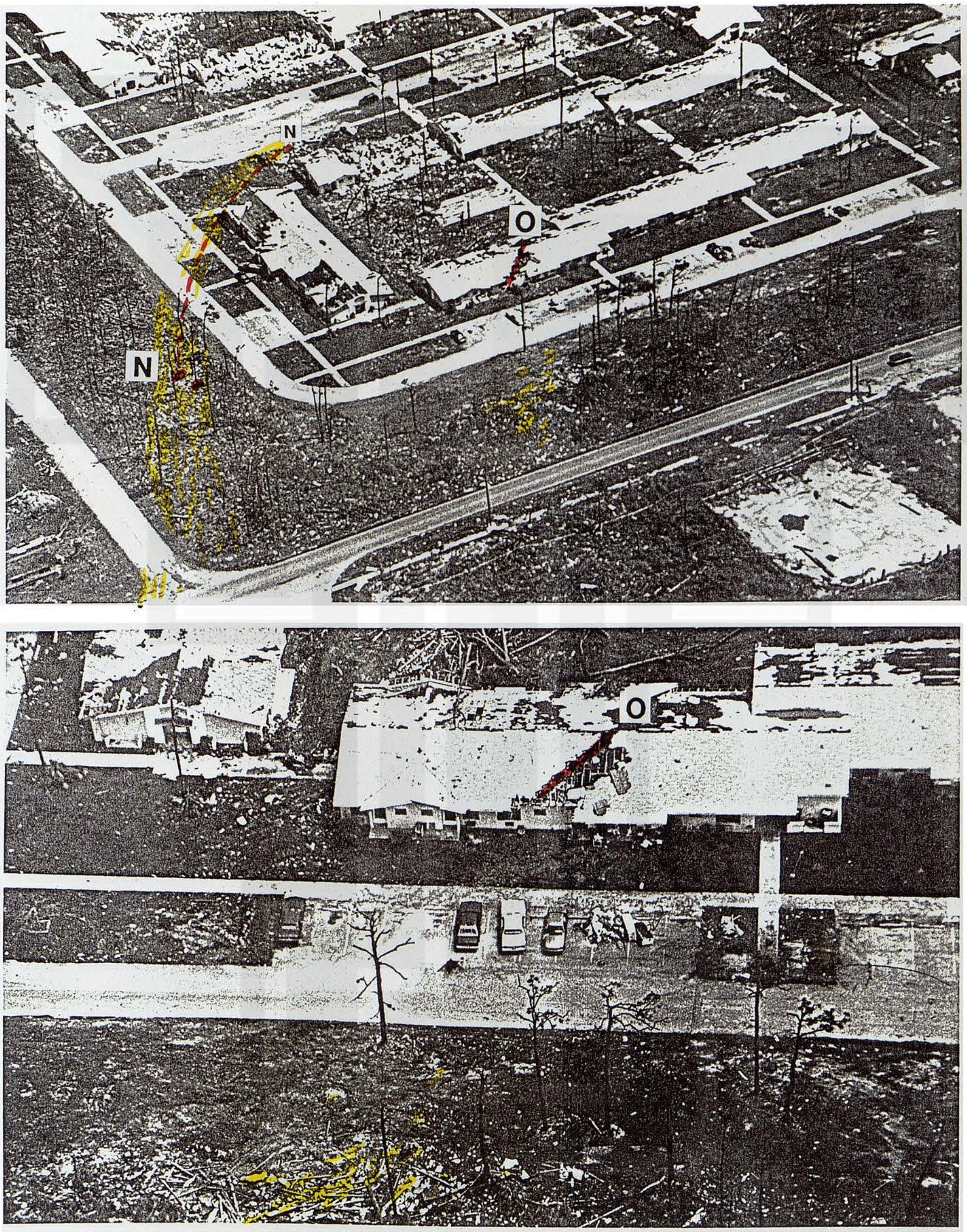

Fig. 6.5 Aerial photo of the debris and a dumpster from **N**. A sharp cut by a falling tie beam is seen at **O**.

N O

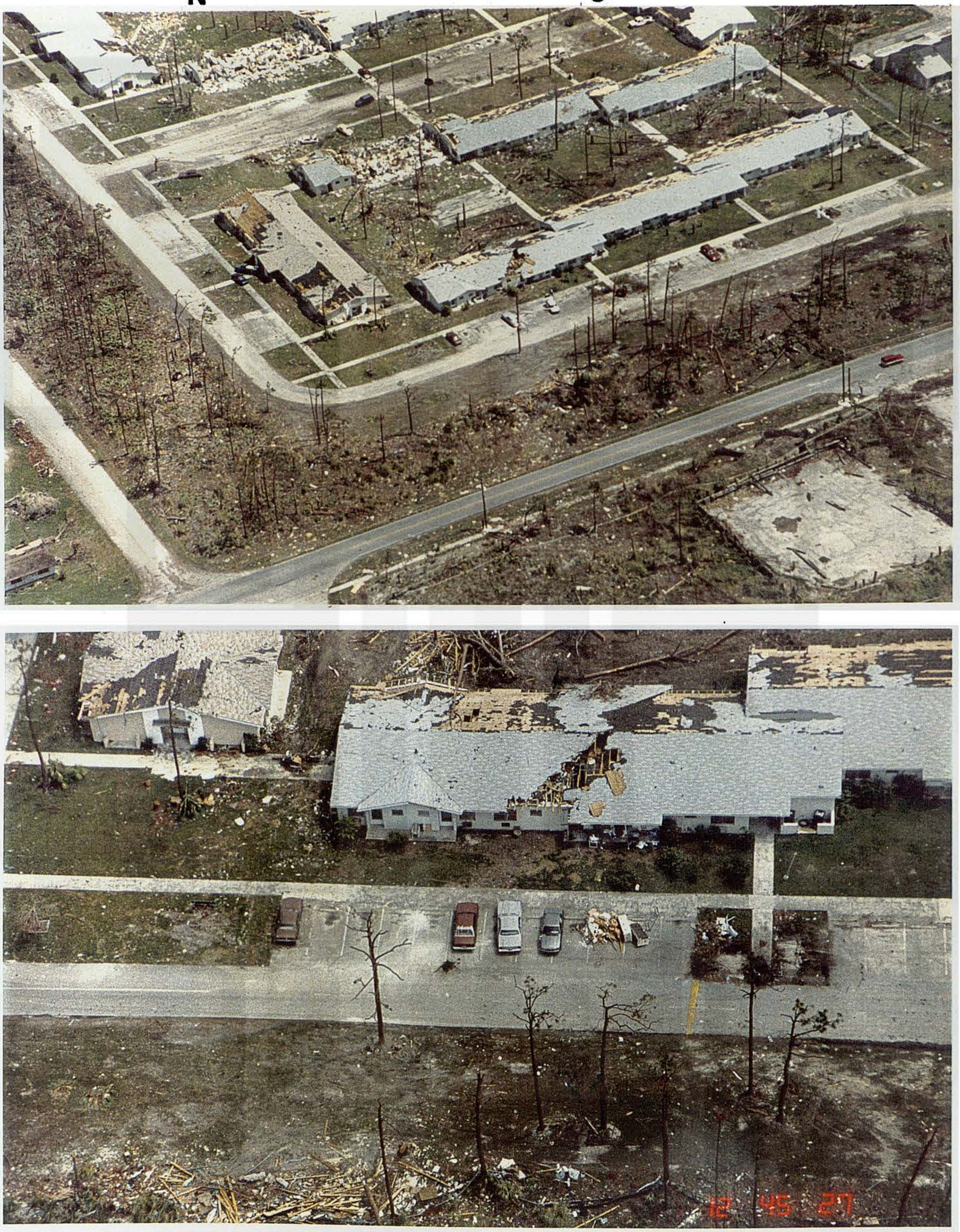

Fig. 6.6 Aerial color pictures of Figure 6.5 taken by Fujita.

Fig. 6.7 Estimated trajectory of dumpster **N** which flew through an estimated distance of 110 meters (360 feet). The winds were induced by an anticyclonic mini-swirl inside the first winds.

N

Fig. 6.8 Aerial color photo of Figure 6.7 taken by Fujita.

P

Fig. 6.9 A ground picture taken by Fujita, showing a complicated pattern of winds. For the picture location, refer to the index picture in Figure 6.10. The photo was taken facing toward the west-southwest.

MINI-SWIRLS AT PINE WOODS VILLA

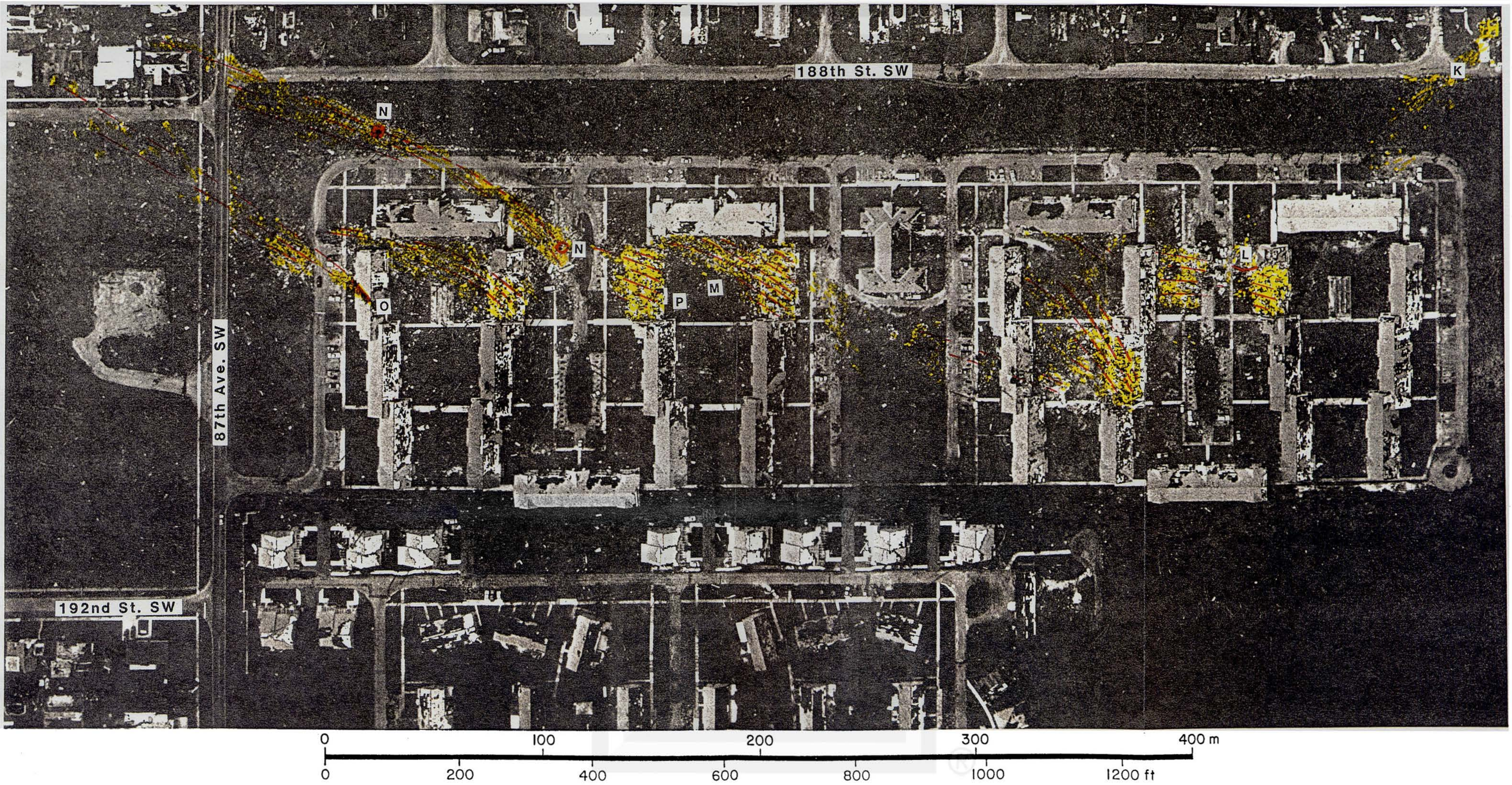

Fig 6.10 An aerial photo of Pine Woods Villa, known to local people as "hot housing" constructed for senior citizens.